

(Supplementary Information): Understanding the changes in thermoelectric properties of bournonite, CuPbSbS_3 , with substitutions.

Alireza Faghaninia^{†,*}, Guodong Yu[¶], Umut Aydemir[§], Max Wood[§], Wei Chen[¶], Gian-Marco Rignanese[¶], G. Jeffrey Snyder[§], Geoffroy Hautier[¶], and Anubhav Jain^{†,*}

[†] Energy Technologies Area, Lawrence Berkeley National Lab, 1 Cyclotron Rd, Berkeley, CA, USA

[§] Department of Materials Science and Engineering, Northwestern University, 2220 Campus Drive, Evanston, IL, USA

[¶] Institute of Condensed Matter and Nanosciences (IMCN), Université catholique de Louvain, Chemin des étoiles 8, bte L7.03.01, Louvain-la-Neuve, Belgium

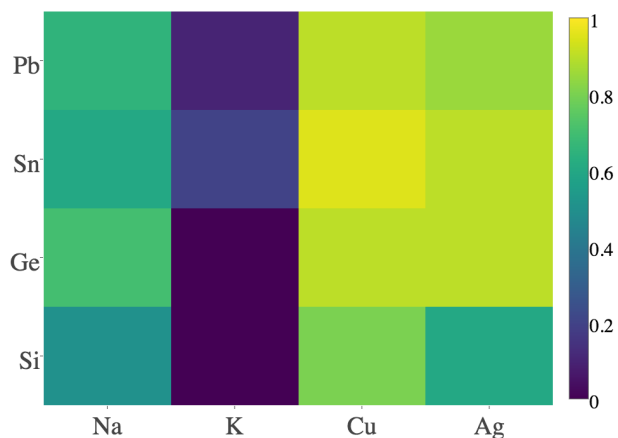
* E-mail: alireza.faghaninia@gmail.com, ajain@lbl.gov

Table of Contents

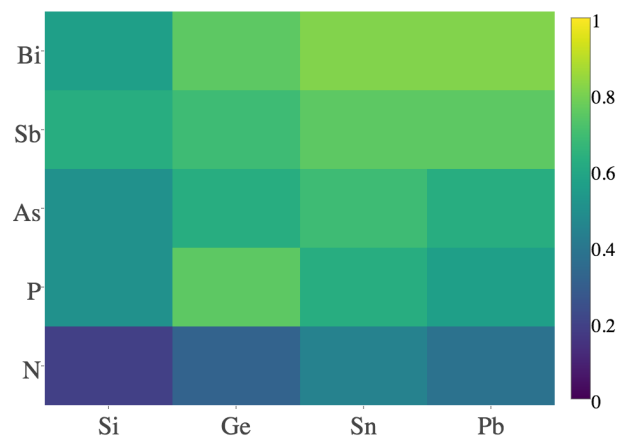
1	Heatmaps: Fraction of compounds that result in bournonite-type structure	2
2	Band Structures: projected band structures and band gap statistics	3
3	Defects: intrinsic for CuPbSbS_3, CuPbSbSe_3, CuSnSbSe_3 and extrinsic for CuPbSbS_3.....	5
4	Intra-group changes in properties (detailed): E_{form}, E_h, E_g, n-PF, p-PF	14
5	Comparison of predicted transport properties via AMSET and BoltzTraP.....	24
6	Heatmaps: how properties change within two groups	25

1 Heatmaps: Fraction of compounds that result in bournonite-type structure

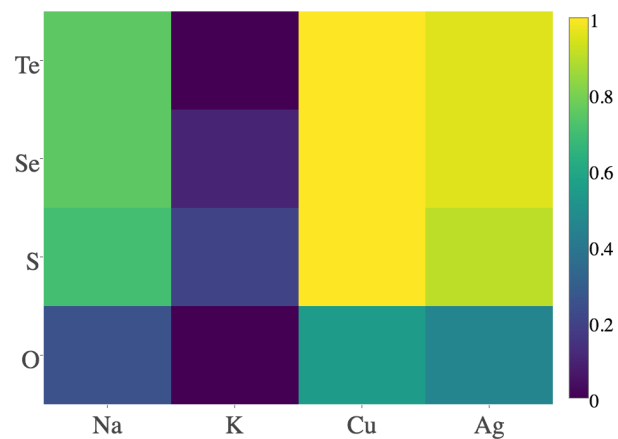
N P As Sb Bi , O S Se Te fixed: bournonite type



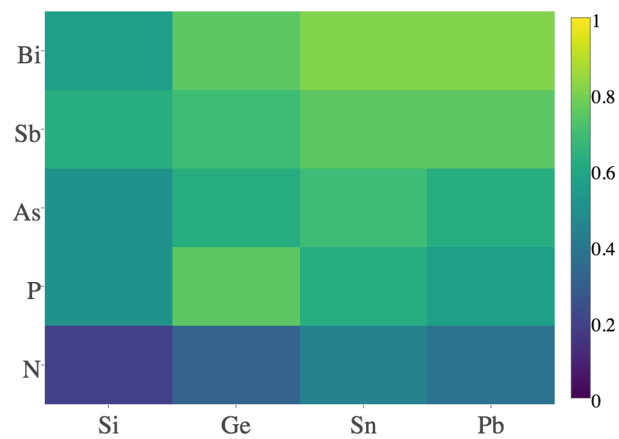
Na K Cu Ag , O S Se Te fixed: bournonite type



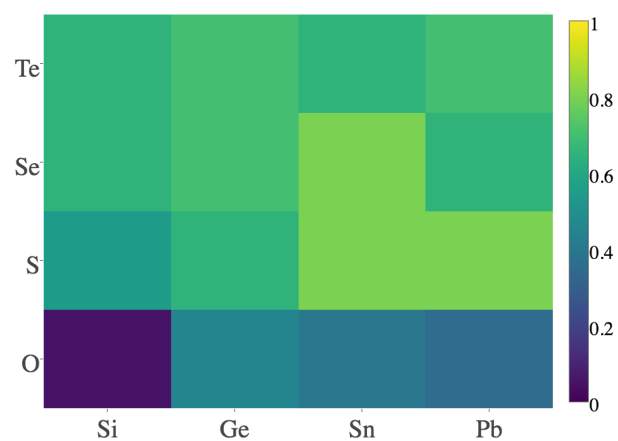
Si Ge Sn Pb , N P As Sb Bi fixed: bournonite type



Na K Cu Ag , O S Se Te fixed: bournonite type



Na K Cu Ag , N P As Sb Bi fixed: bournonite type



Na K Cu Ag , Si Ge Sn Pb fixed: bournonite type

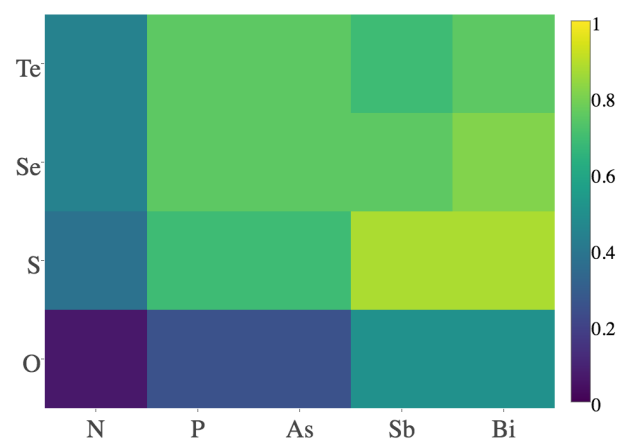


Figure S1. The fraction of compounds that relax into a bournonite-type structure (see the manuscript for definition). Note that compounds containing K almost never relaxes to a bournonite structure and those containing O rarely do so.

2 Band Structures: projected band structures and band gap statistics

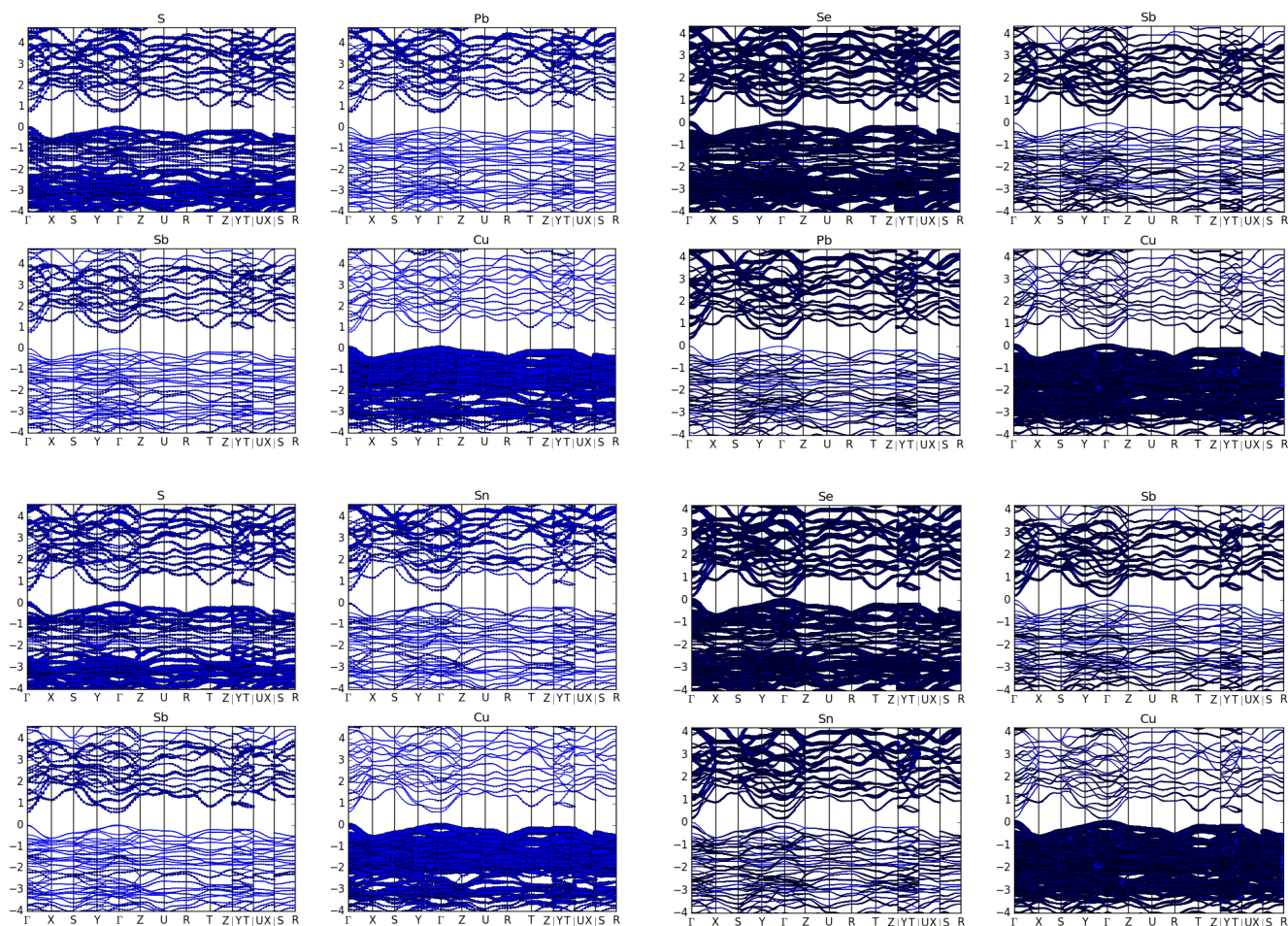


Figure S2. Comparing the band structures and their atomic projections for CuPbSbS3 (top-left), CuPbSbSe (top-right), CuSnSbS3 (bottom-left) and CuSnSbSe3 (bottom-right).

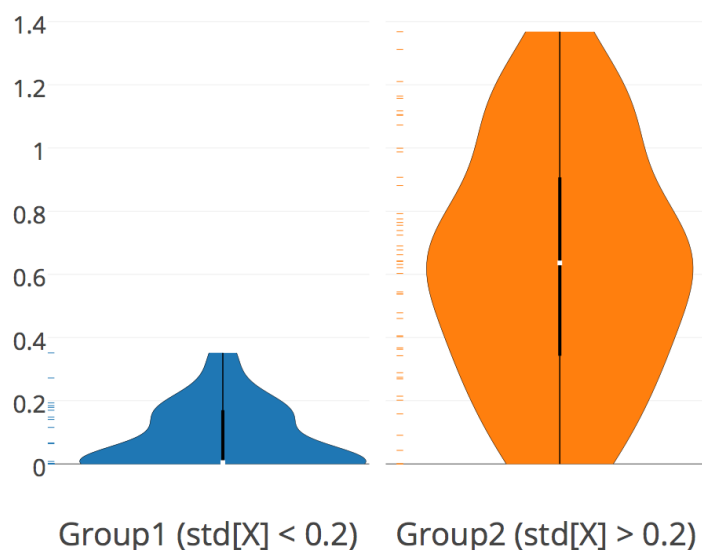
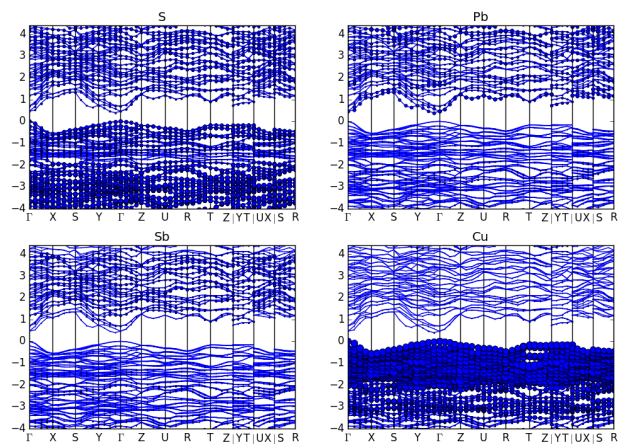
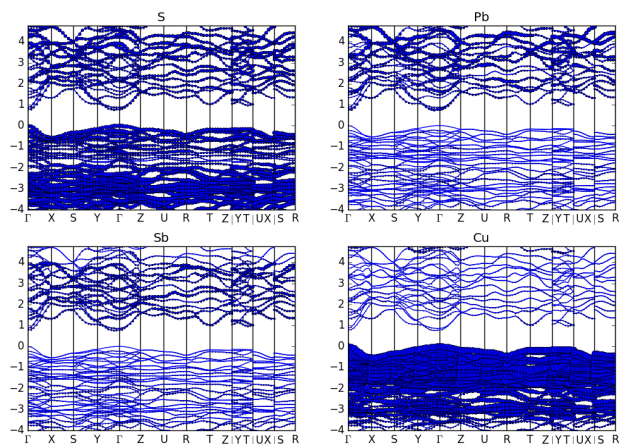


Figure S3. Distribution of calculated band gaps for elements that tend to be relatively stable in bourmonite (i.e., excluding Na, K, Si, N, and O), there appear to be two broad groups of bourmonite materials. Group 1 are large unit cells with relatively low electronegativity differences ($>725 \text{ \AA}^3$ cells with standard deviation of electronegativity <0.2). Group 2 are smaller unit cells with medium electronegativity differences ($<725 \text{ \AA}^3$ cells with standard deviation of electronegativity >0.2).

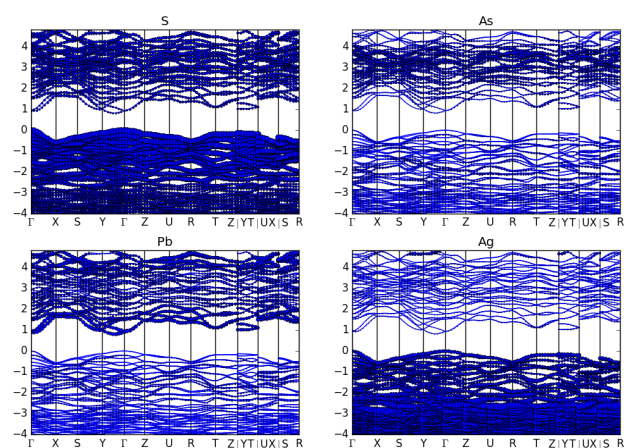
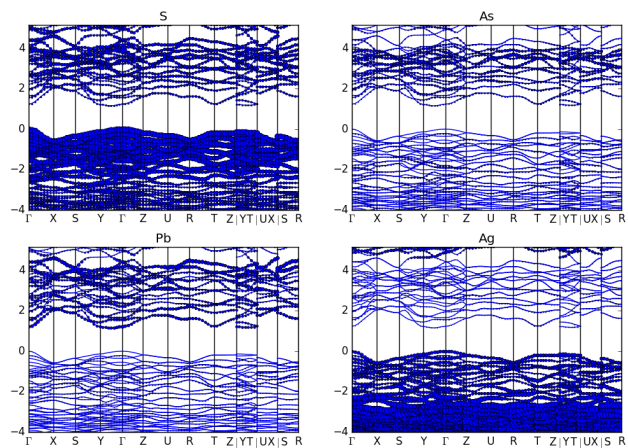
no SOC

SOC

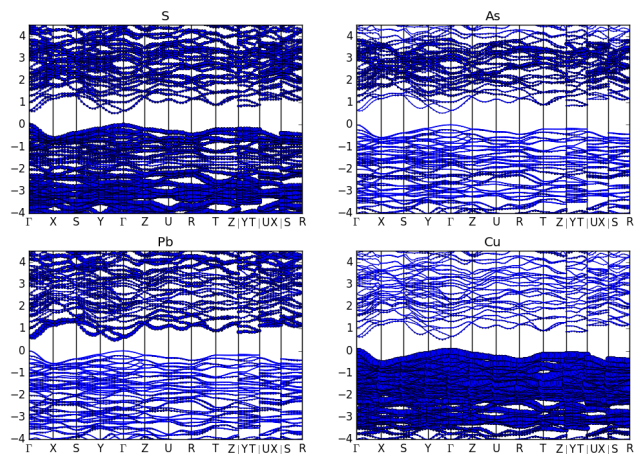
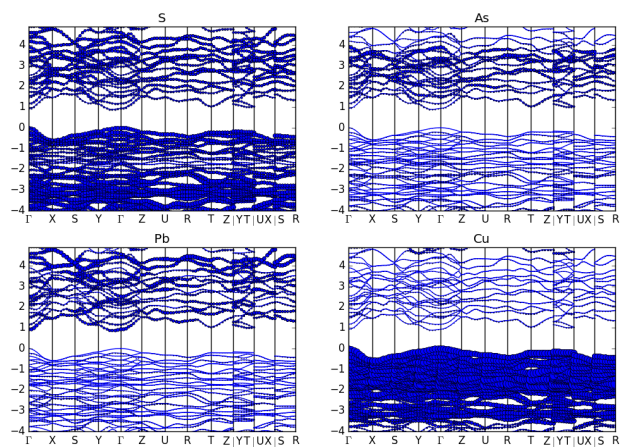
CuPbSbS₃



AgPbAsS₃



CuPbAsS₃



CuSnSbS₃

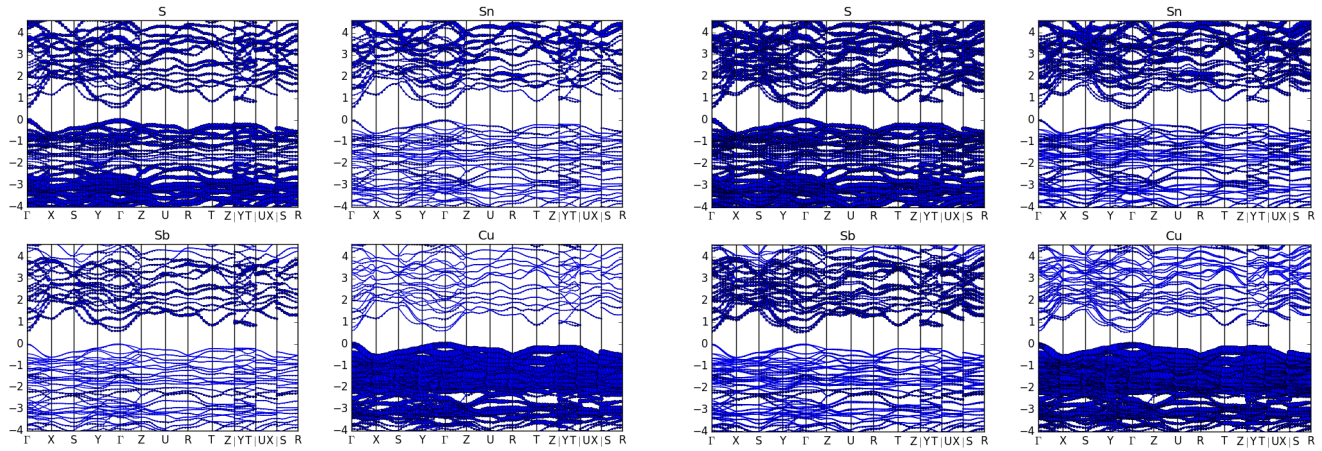


Figure S4. Comparing the band structures without (left) and with (right) spin orbit coupling (SOC) contributions. It is noteworthy that only the conduction bands hence n-type transport properties are significantly affected when SOC is included, but valence bands (and hence *p*-type power factors are largely unaffected by spin-orbit coupling.

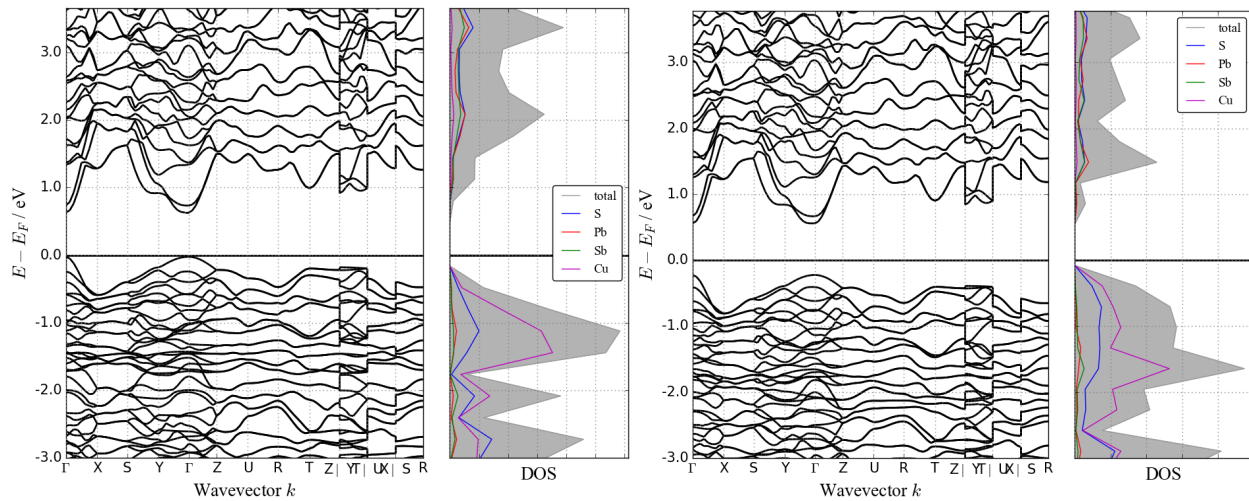
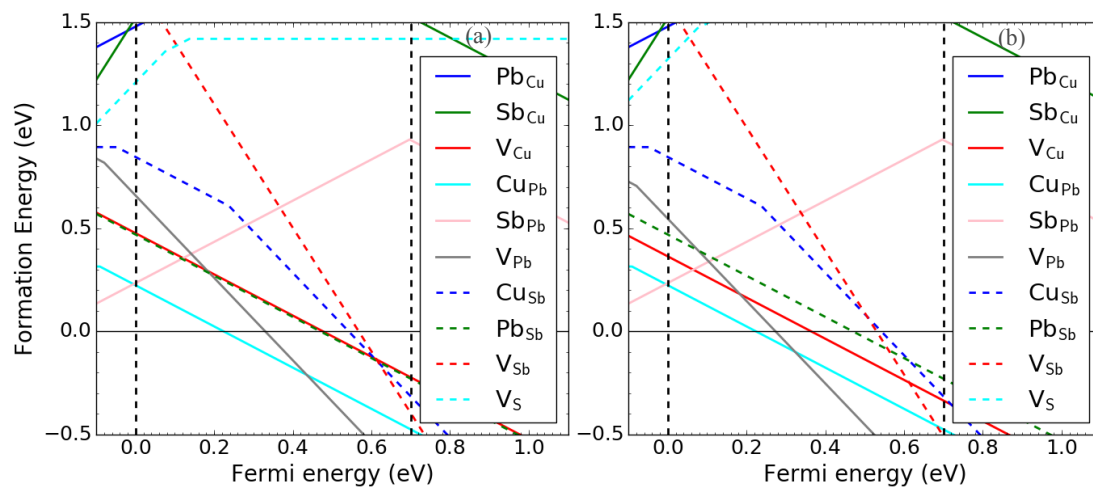


Figure S5. The band structure and atom-projected density of states of bournonite (CuPbSbS₃) with GGA (left) and GGA+U (right, U=3) functionals. Although the band gap increases (0.66 vs. 0.78 eV) upon the use of GGA+U, the Cu-d states remain dominant in the valence band.

3 Defects: intrinsic for CuPbSbS₃, CuPbSbSe₃, CuSnSbSe₃ and extrinsic for CuPbSbS₃



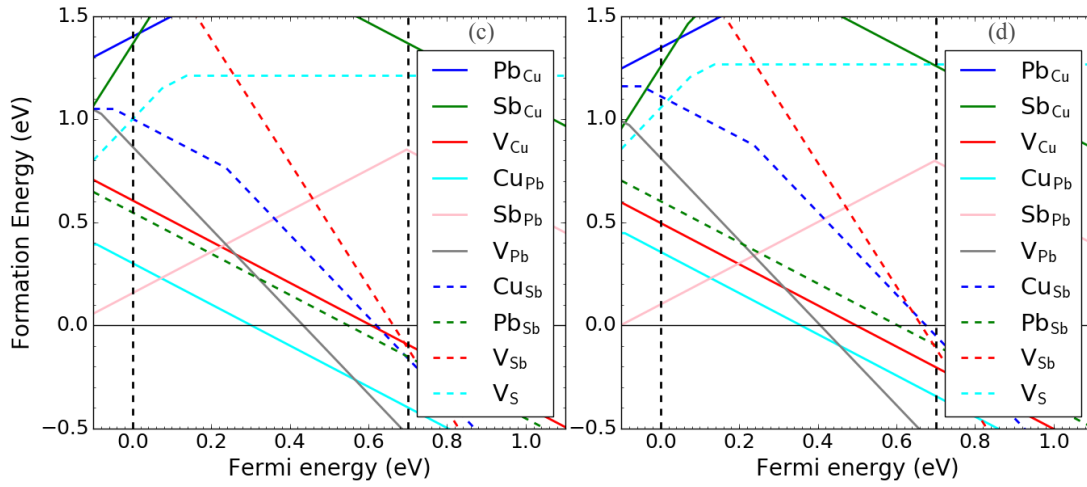


Figure S6. Formation energies of intrinsic defects in CuPbSbS_3 in different regions of phase diagram followed by the chemical potential in eV of each element in this region:

- (a) $\text{Cu}_3\text{SbS}_4\text{-Cu}_{12}\text{Sb}_4\text{S}_{13}\text{-CuSbS}_2\text{-PbS}$ {Pb: -4.501, Sb: -4.41, S: -4.413, Cu: -4.233}
- (b) $\text{Cu}_3\text{SbS}_4\text{-Sb}_8(\text{PbS}_5)_3\text{-CuSbS}_2\text{-PbS}$ {Pb: -4.614, Sb: -4.523, S: -4.3, Cu: -4.346}
- (c) $\text{Cu}_{12}\text{Sb}_4\text{S}_{13}\text{-CuSbS}_2\text{-PbS-Sb}$ {Pb: -4.293, Sb: -4.124, S: -4.621, Cu: -4.103}
- (d) $\text{Sb}_8(\text{PbS}_5)_3\text{-CuSbS}_2\text{-PbS-Sb}$ {Pb: -4.348, Sb: -4.124, S: -4.566, Cu: -4.213}

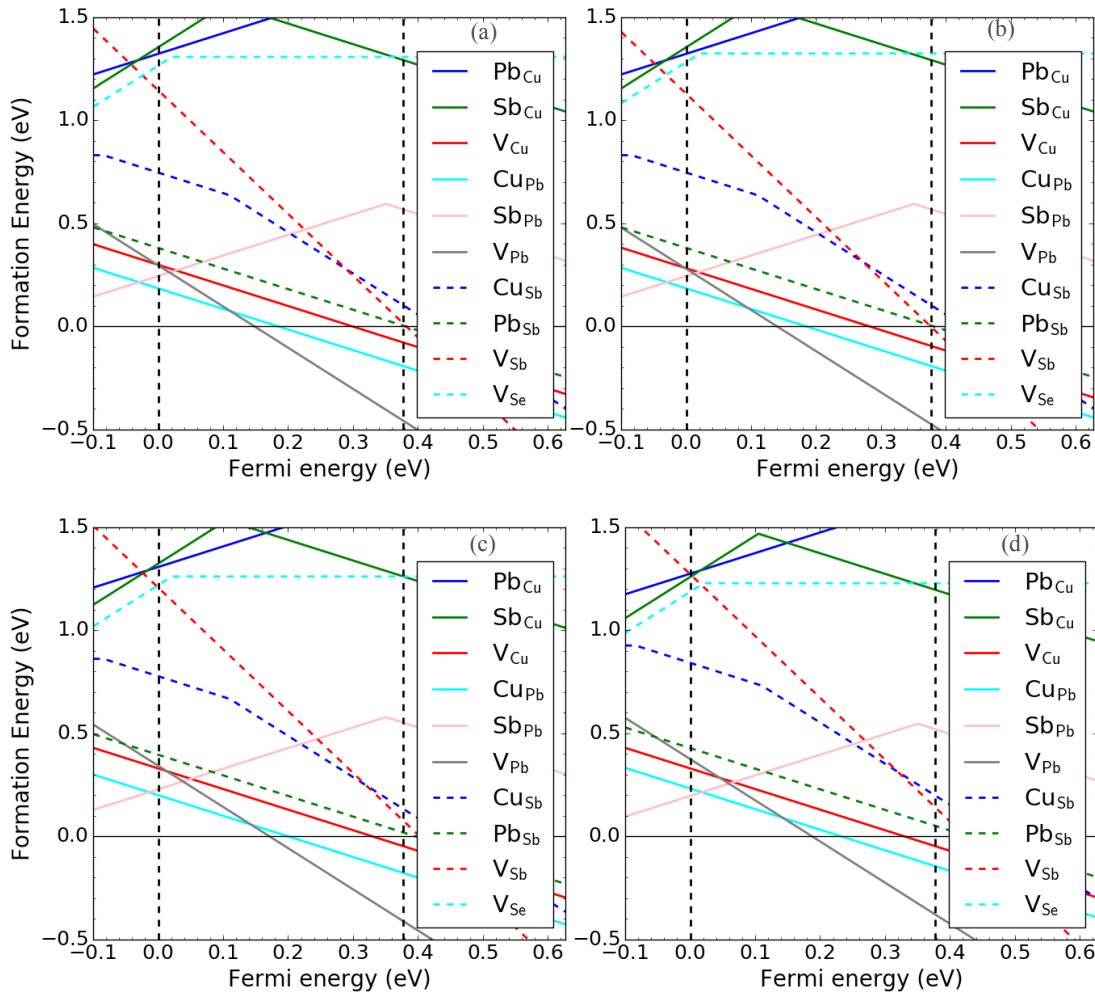


Figure S7. Formation energies of intrinsic defects in CuPbSbSe_3 in different regions of phase diagram followed by the chemical potential in eV of each element in this region:

- (a) $\text{Cu}_3\text{SbSe}_4\text{-Cu}_3\text{Se}_2\text{-CuSbSe}_2\text{-PbSe}$ {Pb: -4.554, Sb: -4.357, Cu: -4.13, Se: -3.775}

- (b) $\text{Cu}_3\text{SbSe}_4\text{-CuSbSe}_2\text{-PbSe-Sb}_2\text{Se}_3$ {Pb: -4.571, Sb: -4.373, Cu: -4.147, Se: -3.758}
 (c) $\text{Cu-Cu}_3\text{Se}_2\text{-CuSbSe}_2\text{-PbSe}$ {Pb: -4.508, Sb: -4.295, Cu: -4.099, Se: -3.821}
 (d) $\text{Cu-CuSbSe}_2\text{-PbSe-Sb}_2\text{Se}_3$ {Pb: -4.475, Sb: -4.23, Cu: -4.099, Se: -3.853}

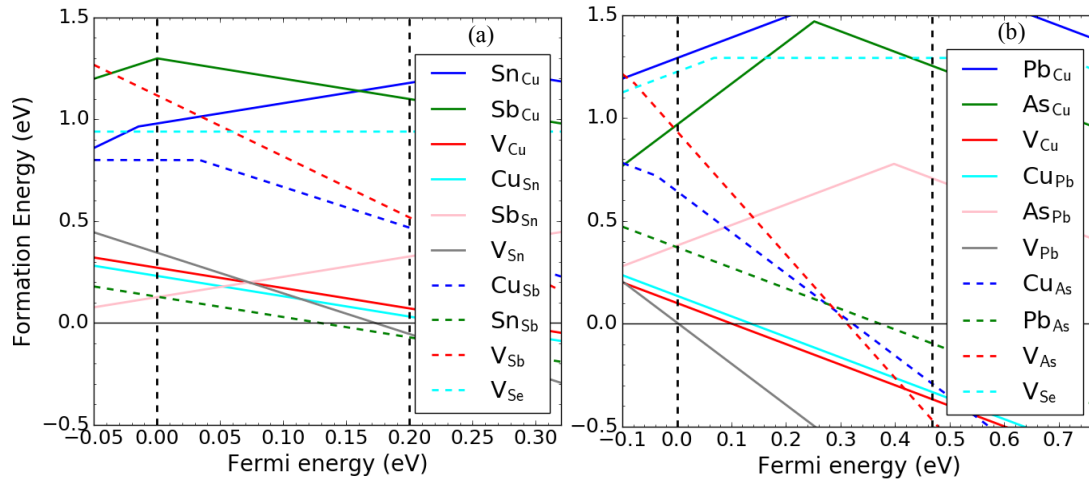
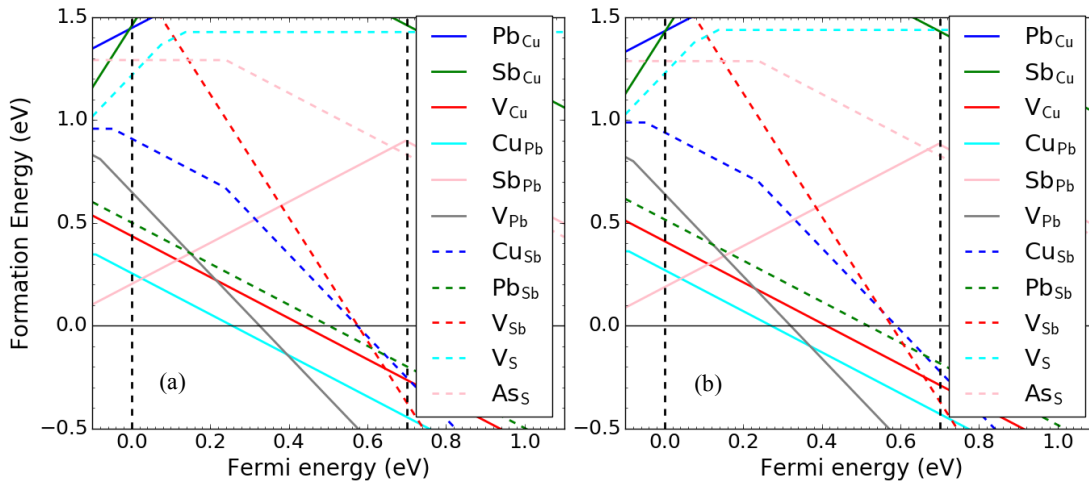
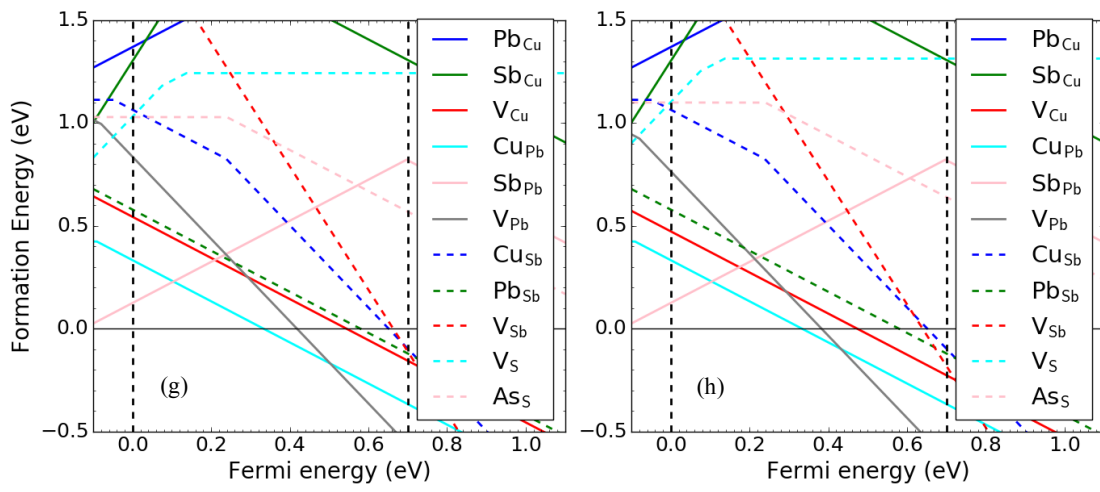
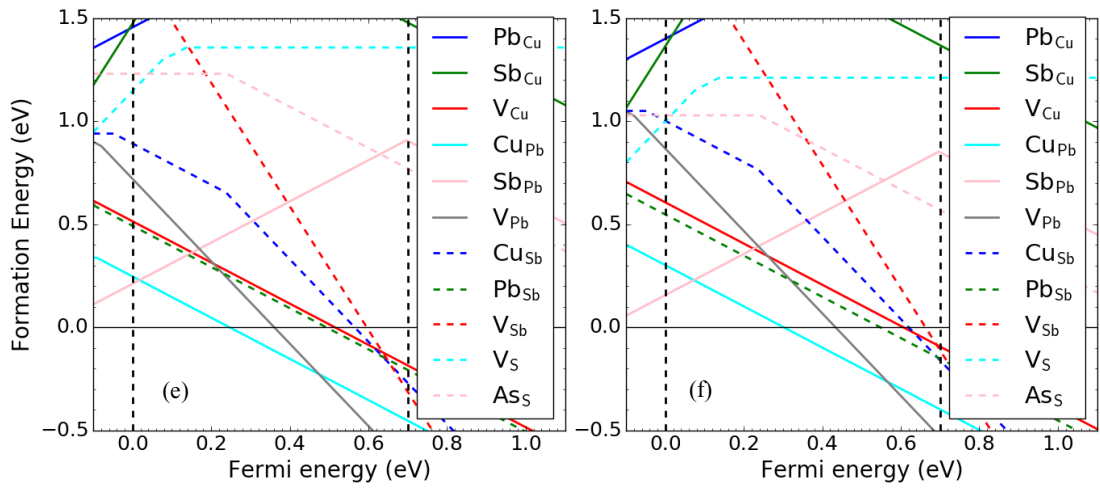
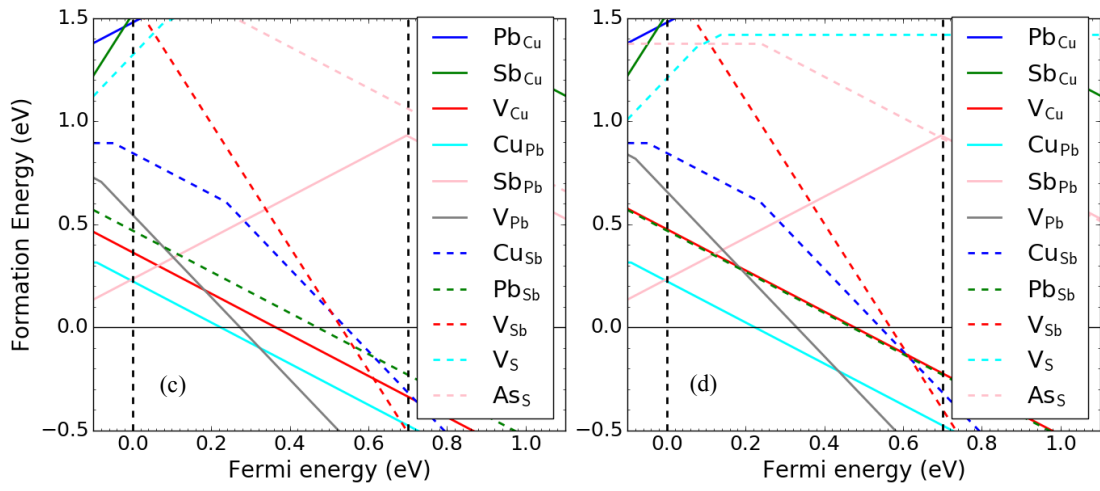


Figure S8. Formation energies of intrinsic defects in a) CuSnSbSe_3 and b) CuPbAsSe_3 with chemical potentials chosen at only one region of phase diagram. Chemical potential is in eV unit. Two dashed vertical lines are VBM and CBM respectively.

- (a) CuSnSbSe_3 at $\text{Cu-Cu}_2\text{SnSe}_3\text{-Sb}_2\text{Se}_3\text{-SnSe}$ region, where chemical potentials are { Cu: -4.099, Sn: -4.465, Sb: -4.16, Se: -3.9} .
 (b) CuPbAsSe_3 at $\text{As}_2\text{Se}_3\text{-Cu}_3\text{AsSe}_4\text{-CuAsSe-PbSe}$ region, where chemical potentials are { Cu: -4.27, Pb: -4.68, As: -4.71, Se: -3.64}





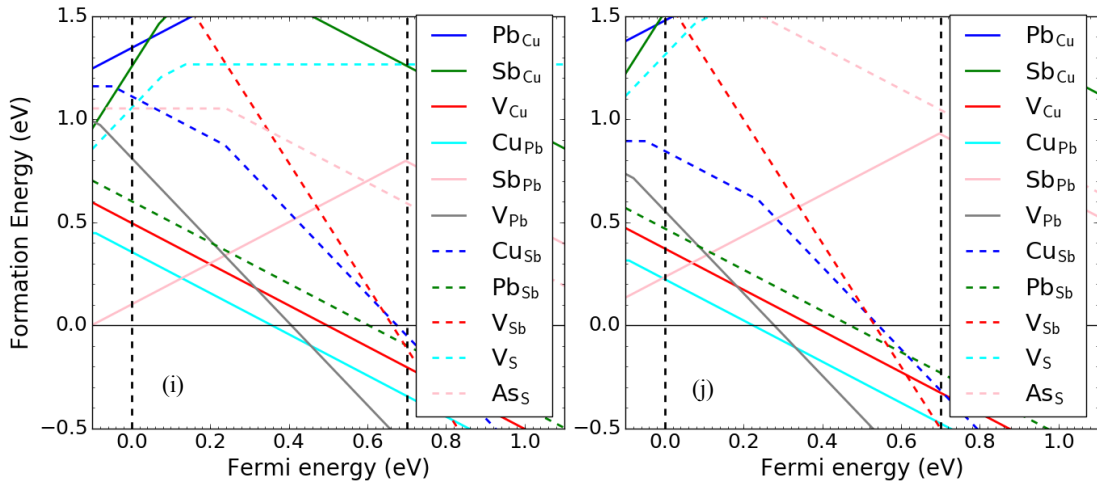


Figure S9. Formation energies of defects in CuPbSbS_3 including extrinsic impurity As on S in different regions of phase diagram followed by the chemical potential in eV of each element in this region:

- (a) $\text{Cu}_6\text{As}_4\text{S}_9\text{-CuAsS-Cu}_{12}\text{As}_4\text{S}_{13}\text{-CuSbS}_2\text{-PbS}$ {Pb: -4.51, Sb: -4.387, S: -4.404, As: -4.736, Cu: -4.273}
- (b) $\text{Cu}_6\text{As}_4\text{S}_9\text{-Sb}_8(\text{PbS}_5)_3\text{-CuAsS-CuSbS}_2\text{-PbS}$ {Pb: -4.52, Sb: -4.382, S: -4.394, As: -4.72, Cu: -4.299}
- (c) $\text{Cu}_6\text{As}_4\text{S}_9\text{-Sb}_8(\text{PbS}_5)_3\text{-CuSbS}_2\text{-Cu}_3\text{SbS}_4\text{-PbS}$ {Pb: -4.614, Sb: -4.523, S: -4.3, As: -4.861, Cu: -4.346}
- (d) $\text{Cu}_{12}\text{Sb}_4\text{S}_{13}\text{-Cu}_{12}\text{As}_4\text{S}_{13}\text{-CuSbS}_2\text{-Cu}_3\text{SbS}_4\text{-PbS}$ {Pb: -4.501, Sb: -4.41, S: -4.413, As: -4.829, Cu: -4.233}
- (e) $\text{CuAsS-Cu}_{12}\text{Sb}_4\text{S}_{13}\text{-Cu}_{12}\text{As}_4\text{S}_{13}\text{-CuSbS}_2\text{-PbS}$ {Pb: -4.44, Sb: -4.326, S: -4.474, As: -4.744, Cu: -4.195}
- (f) $\text{CuAsS-Cu}_{12}\text{Sb}_4\text{S}_{13}\text{-CuSbS}_2\text{-Sb-PbS}$ {Pb: -4.293, Sb: -4.124, S: -4.621, As: -4.689, Cu: -4.103}
- (g) $\text{CuAsS-CuSbS}_2\text{-Sb-As-PbS}$ {Pb: -4.324, Sb: -4.124, S: -4.59, As: -4.658, Cu: -4.165}
- (h) $\text{Sb}_8(\text{PbS}_5)_3\text{-CuAsS-CuSbS}_2\text{-As-PbS}$ {Pb: -4.395, Sb: -4.195, S: -4.519, As: -4.658, Cu: -4.236}
- (i) $\text{Sb}_8(\text{PbS}_5)_3\text{-CuSbS}_2\text{-Sb-As-PbS}$ {Pb: -4.348, Sb: -4.124, S: -4.566, As: -4.658, Cu: -4.213}
- (j) $\text{Cu}_6\text{As}_4\text{S}_9\text{-Cu}_{12}\text{As}_4\text{S}_{13}\text{-CuSbS}_2\text{-Cu}_3\text{SbS}_4\text{-PbS}$ {Pb: -4.605, Sb: -4.514, S: -4.309, As: -4.855, Cu: -4.337}

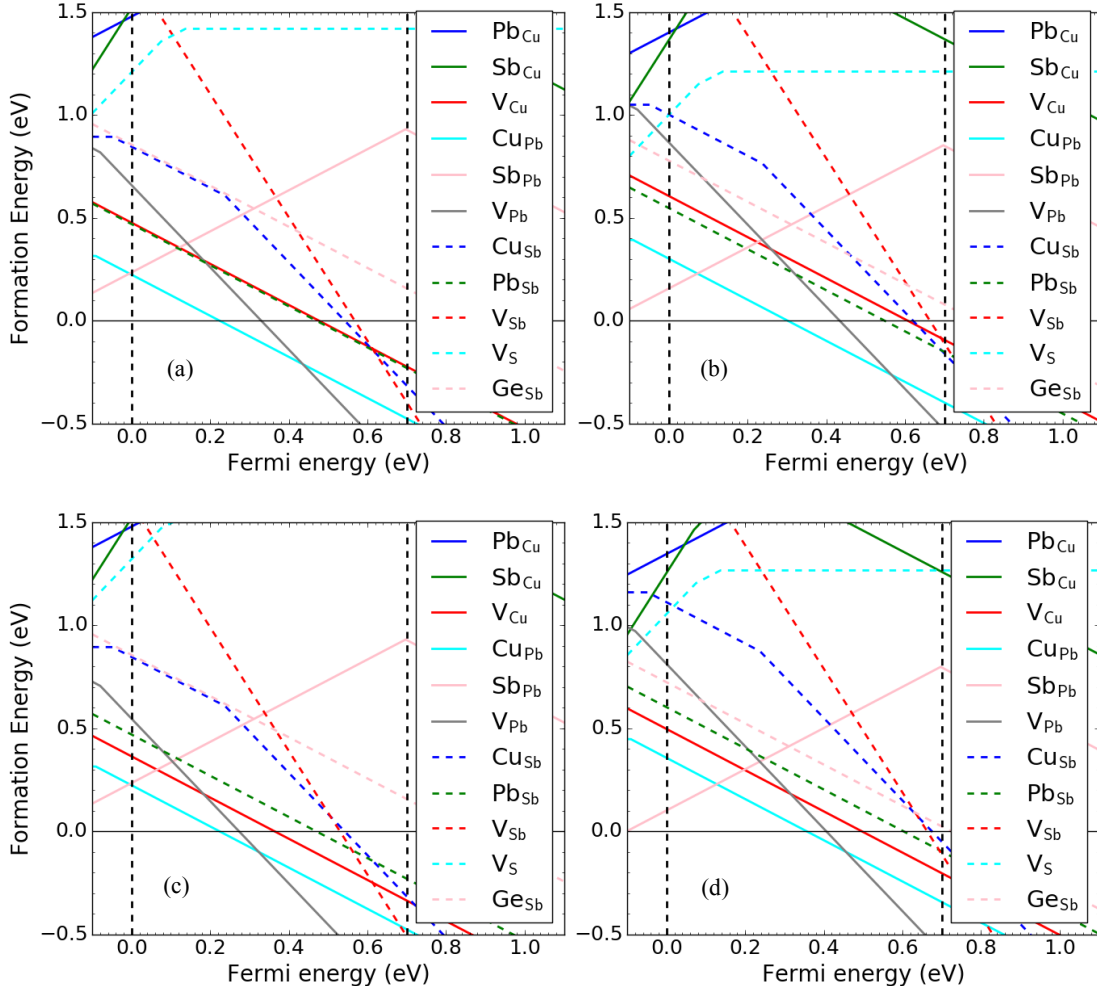


Figure S10. Formation energies of defects in CuPbSbS_3 including extrinsic impurity Ge on Sb in different regions of phase diagram followed by the chemical potential in eV of each element in this region:

- (a) $\text{Cu}_2\text{GeS}_3\text{-Cu}_{12}\text{Sb}_4\text{S}_{13}\text{-CuSbS}_2\text{-Cu}_3\text{SbS}_4\text{-PbS}$ {Pb: -4.501, Sb: -4.41, S: -4.413, Ge: -5.438, Cu: -4.233}
 (b) $\text{Cu}_2\text{GeS}_3\text{-Cu}_{12}\text{Sb}_4\text{S}_{13}\text{-CuSbS}_2\text{-Sb-PbS}$ {Pb: -4.293, Sb: -4.124, S: -4.621, Ge: -5.074, Cu: -4.103}
 (c) $\text{Sb}_8(\text{PbS}_5)_3\text{-Cu}_2\text{GeS}_3\text{-CuSbS}_2\text{-Cu}_3\text{SbS}_4\text{-PbS}$ {Pb: -4.614, Sb: -4.523, S: -4.3, Ge: -5.55, Cu: -4.346}
 (d) $\text{Sb}_8(\text{PbS}_5)_3\text{-Cu}_2\text{GeS}_3\text{-CuSbS}_2\text{-Sb-PbS}$ {Pb: -4.348, Sb: -4.124, S: -4.566, Ge: -5.019, Cu: -4.213}

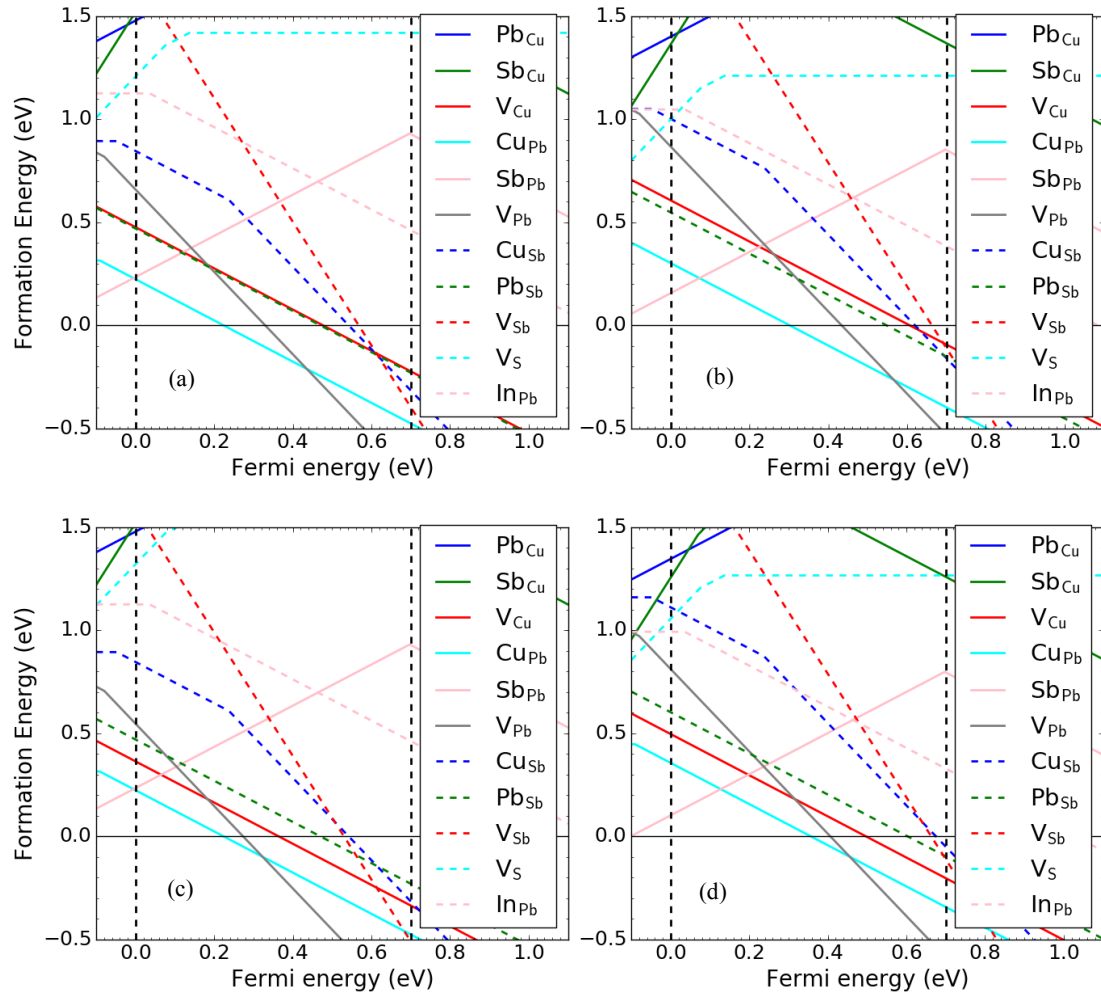
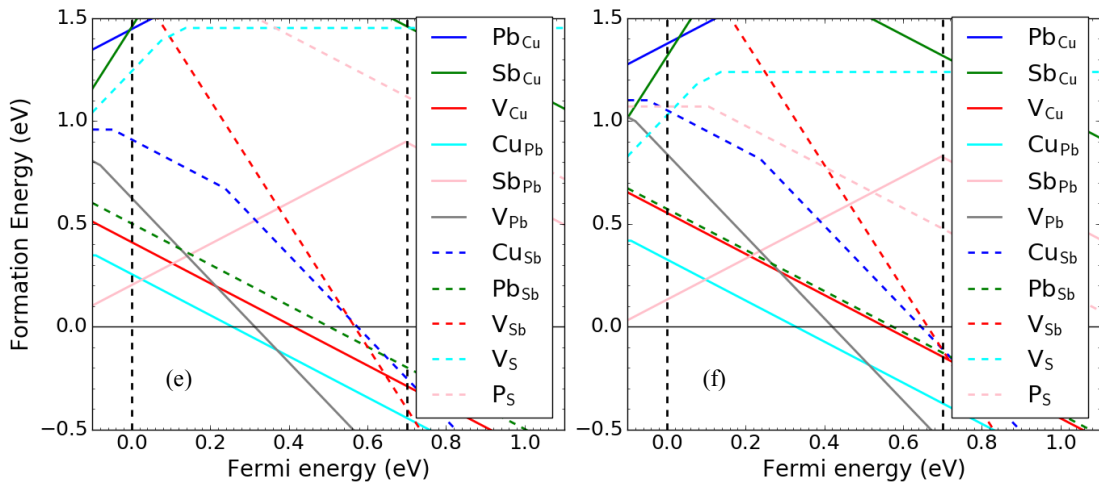
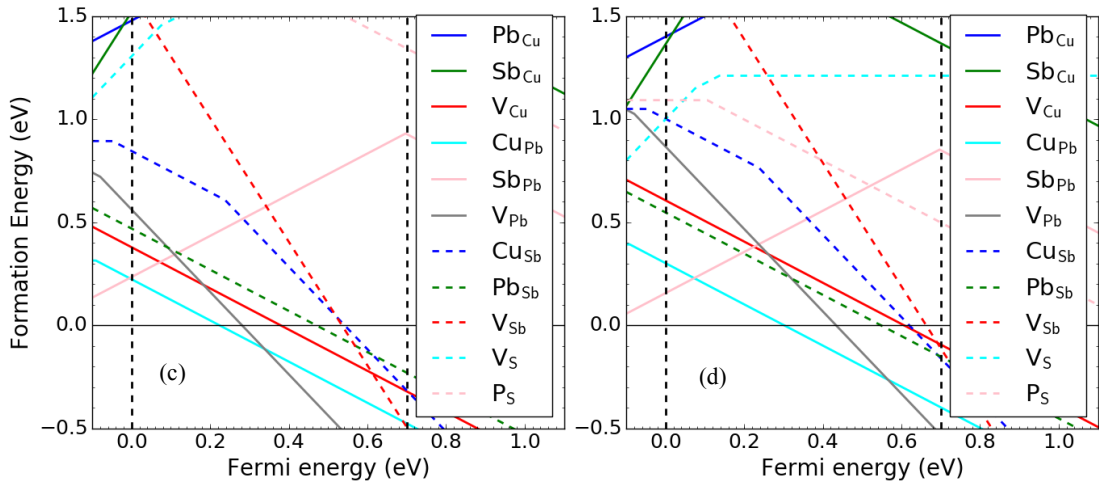
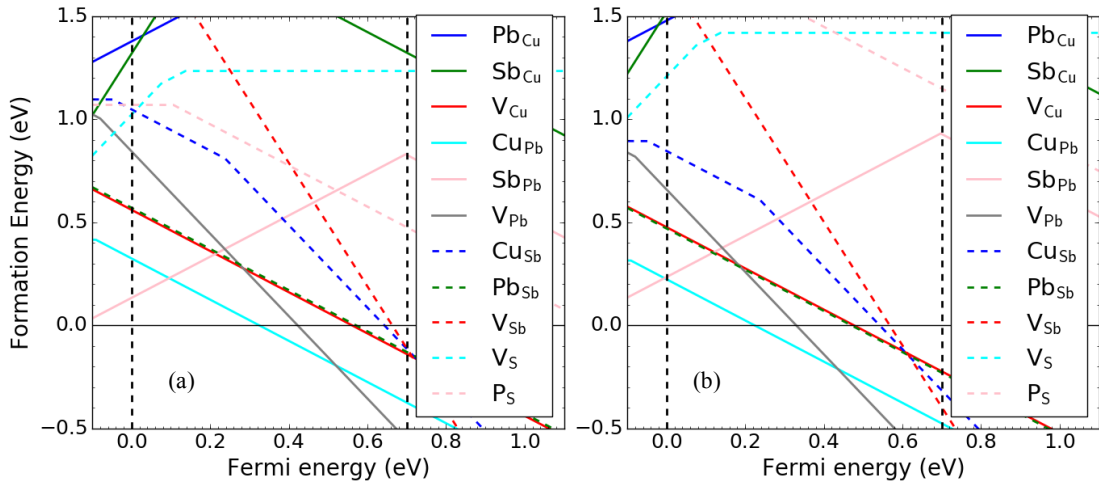


Figure S11. Formation energies of defects in CuPbSbS_3 including extrinsic impurity In on Pb in different regions of phase diagram followed by the chemical potential in eV of each element in this region:

- (a) $\text{InCuS}_2\text{-Cu}_{12}\text{Sb}_4\text{S}_{13}\text{-CuSbS}_2\text{-Cu}_3\text{SbS}_4\text{-PbS}$ {Pb: -4.501, Sb: -4.41, S: -4.413, Cu: -4.233, In: -3.983}
 (b) $\text{InCuS}_2\text{-Cu}_{12}\text{Sb}_4\text{S}_{13}\text{-CuSbS}_2\text{-Sb-PbS}$ {Pb: -4.293, Sb: -4.124, S: -4.621, Cu: -4.103, In: -3.696}
 (c) $\text{InCuS}_2\text{-Sb}_8(\text{PbS}_5)_3\text{-CuSbS}_2\text{-Cu}_3\text{SbS}_4\text{-PbS}$ {Pb: -4.614, Sb: -4.523, S: -4.3, Cu: -4.346, In: -4.095}
 (d) $\text{InCuS}_2\text{-Sb}_8(\text{PbS}_5)_3\text{-CuSbS}_2\text{-Sb-PbS}$ {Pb: -4.348, Sb: -4.124, S: -4.566, Cu: -4.213, In: -3.696}



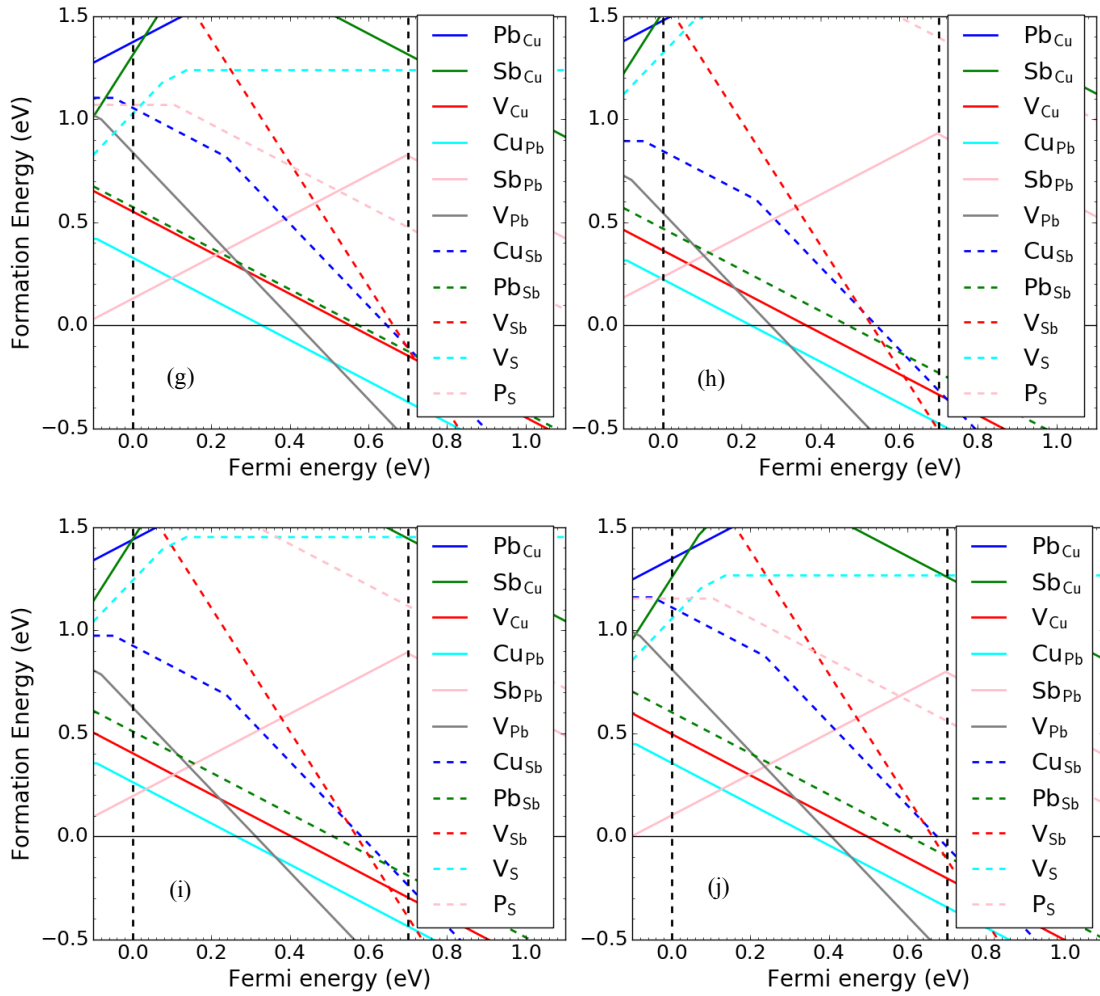


Figure S12. Formation energies of defects in CuPbSbS_3 including extrinsic impurity P on S in different regions of phase diagram followed by the chemical potential in eV of each element in this region:

- (a) $\text{CuSbS}_2\text{-Cu}_3\text{PS}_4\text{-CuP}_2\text{-PbS-Sb}$ {Pb: -4.316, Sb: -4.124, S: -4.598, Cu: -4.149, P: -5.555}
- (b) $\text{CuSbS}_2\text{-Cu}_3\text{SbS}_4\text{-Cu}_{12}\text{Sb}_4\text{S}_{13}\text{-Cu}_3\text{PS}_4\text{-PbS}$ {Pb: -4.501, Sb: -4.41, S: -4.413, Cu: -4.233, P: -6.043}
- (c) $\text{CuSbS}_2\text{-Cu}_3\text{SbS}_4\text{-P}_2\text{Pb}_3\text{S}_8\text{-Cu}_3\text{PS}_4\text{-PbS}$ {Pb: -4.598, Sb: -4.508, S: -4.315, Cu: -4.33, P: -6.141}
- (d) $\text{CuSbS}_2\text{-Cu}_{12}\text{Sb}_4\text{S}_{13}\text{-Cu}_3\text{PS}_4\text{-PbS-Sb}$ {Pb: -4.293, Sb: -4.124, S: -4.621, Cu: -4.103, P: -5.601}
- (e) $\text{CuSbS}_2\text{-P}_2\text{Pb}_3\text{S}_8\text{-PPbS}_3\text{-Cu}_3\text{PS}_4\text{-PbS}$ {Pb: -4.534, Sb: -4.411, S: -4.38, Cu: -4.298, P: -5.98}
- (f) $\text{CuSbS}_2\text{-PPbS}_3\text{-Cu}_3\text{PS}_4\text{-CuP}_2\text{-PbS}$ {Pb: -4.32, Sb: -4.126, S: -4.594, Cu: -4.155, P: -5.552}
- (g) $\text{CuSbS}_2\text{-PPbS}_3\text{-CuP}_2\text{-PbS-Sb}$ {Pb: -4.32, Sb: -4.124, S: -4.594, Cu: -4.157, P: -5.551}
- (h) $\text{Sb}_8(\text{PbS}_5)_3\text{-CuSbS}_2\text{-Cu}_3\text{SbS}_4\text{-P}_2\text{Pb}_3\text{S}_8\text{-PbS}$ {Pb: -4.614, Sb: -4.523, S: -4.3, Cu: -4.346, P: -6.179}
- (i) $\text{Sb}_8(\text{PbS}_5)_3\text{-CuSbS}_2\text{-P}_2\text{Pb}_3\text{S}_8\text{-PPbS}_3\text{-PbS}$ {Pb: -4.534, Sb: -4.404, S: -4.38, Cu: -4.306, P: -5.98}
- (j) $\text{Sb}_8(\text{PbS}_5)_3\text{-CuSbS}_2\text{-PPbS}_3\text{-PbS-Sb}$ {Pb: -4.348, Sb: -4.124, S: -4.566, Cu: -4.213, P: -5.607}

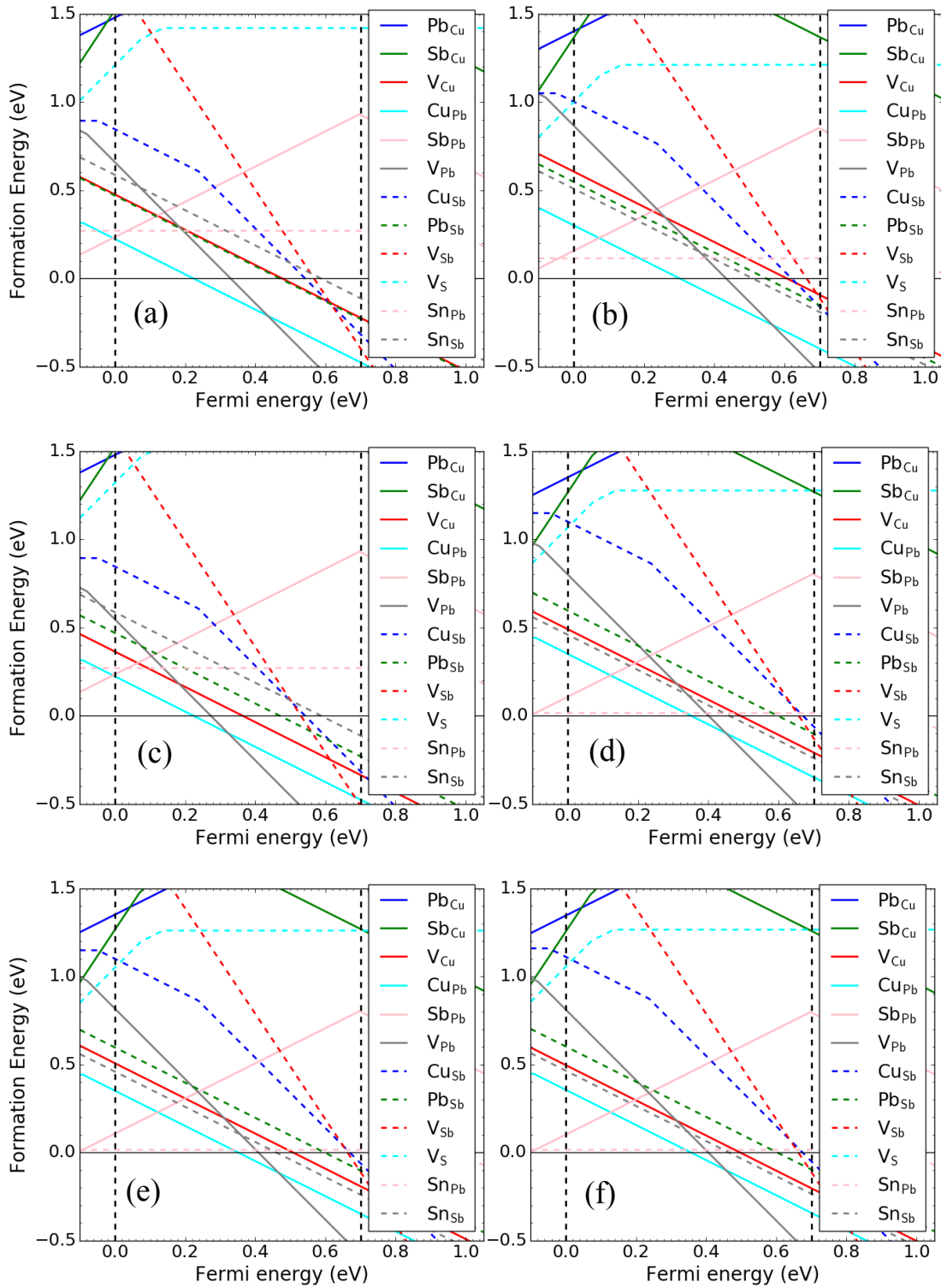
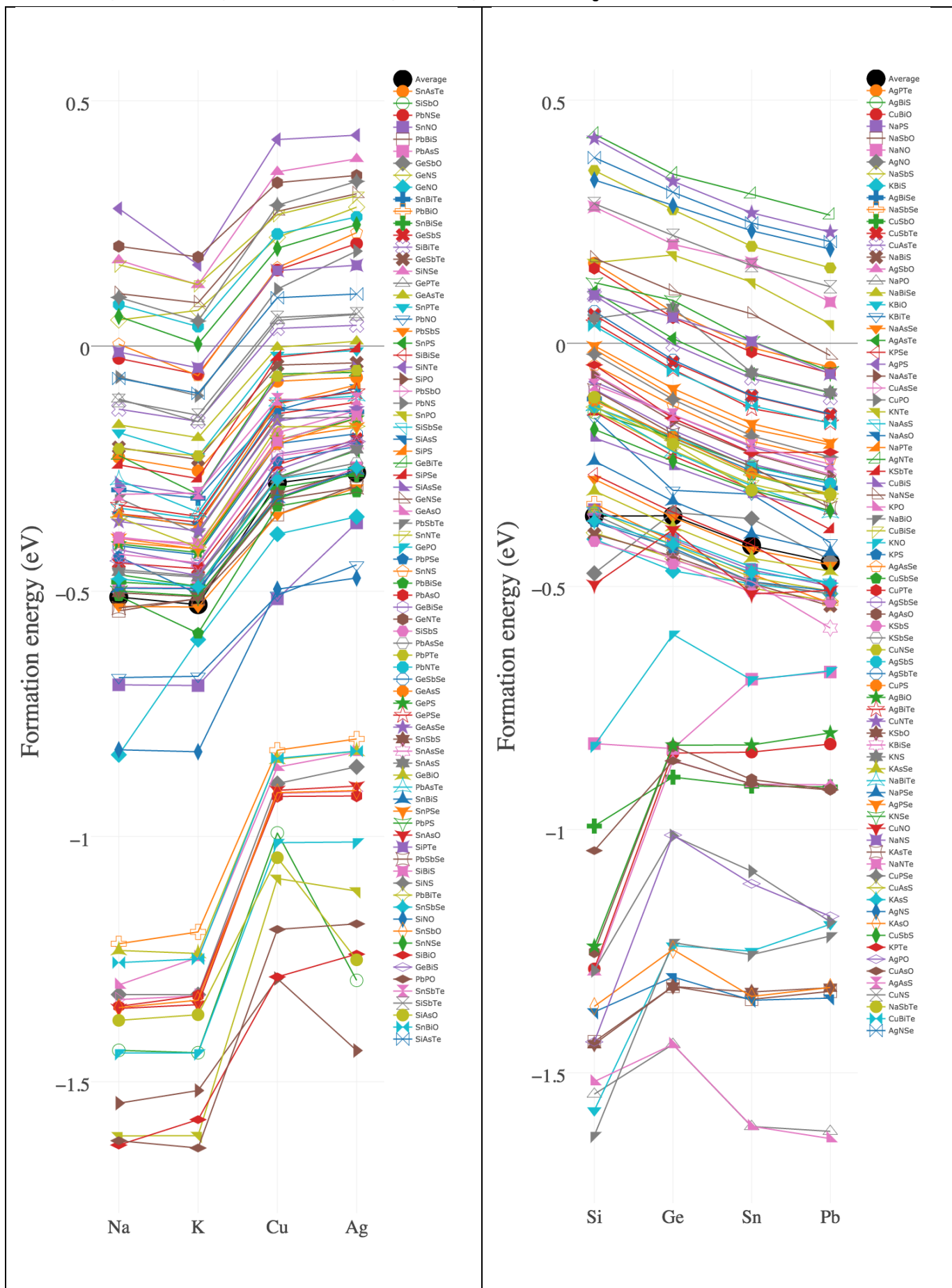
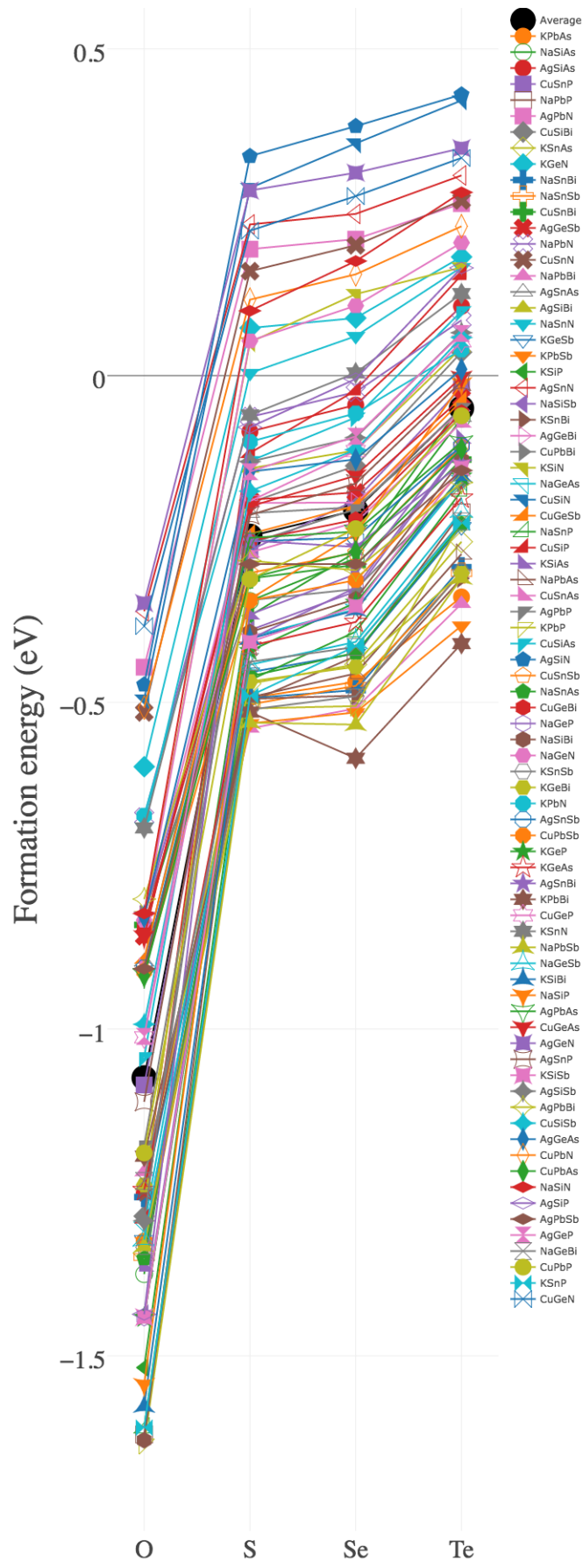
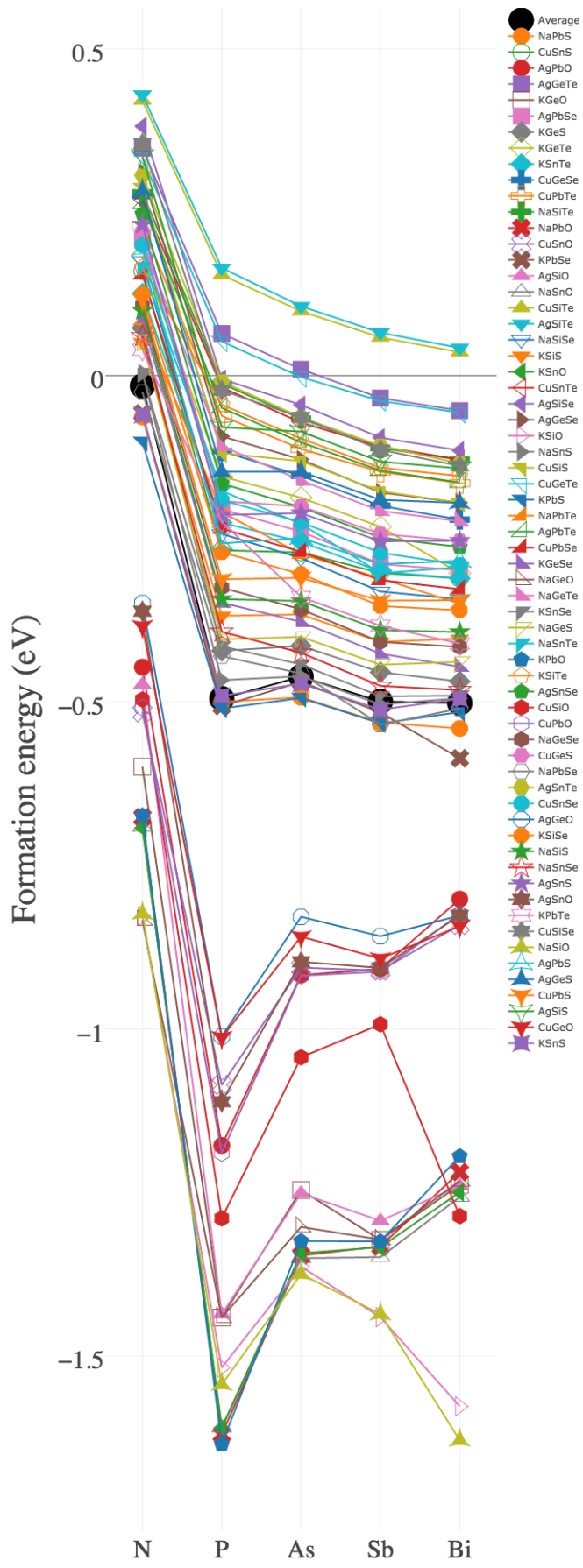


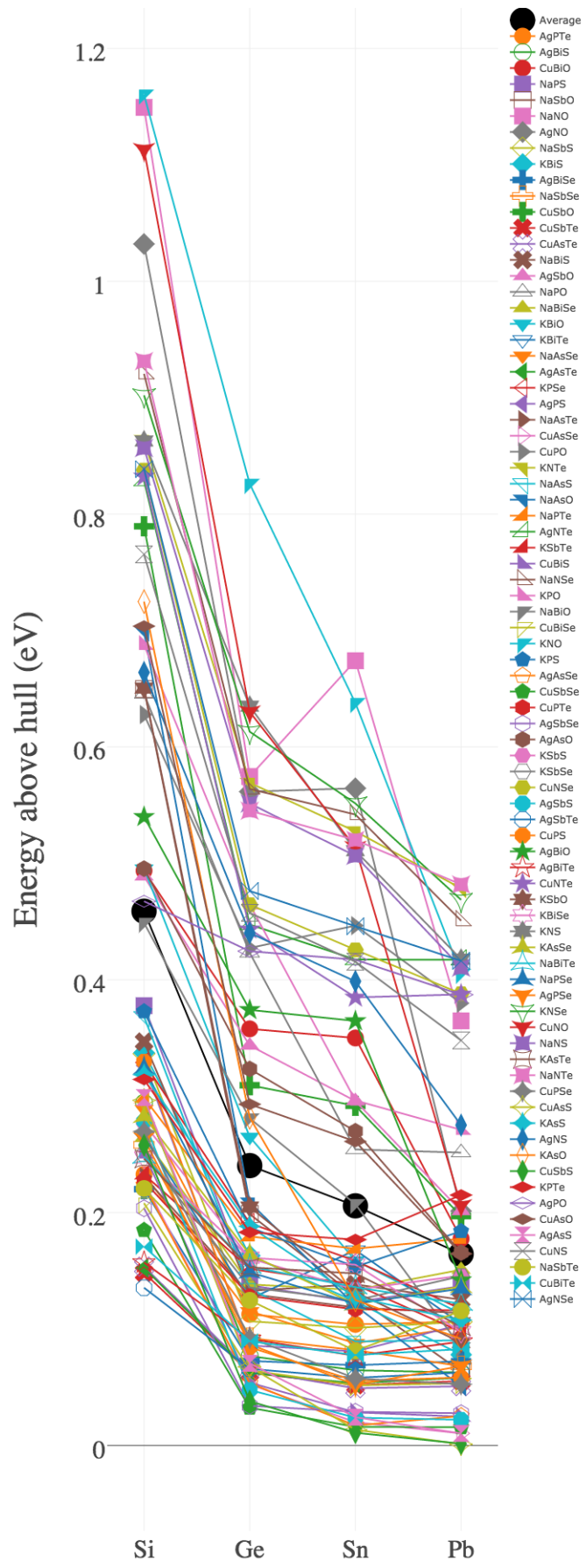
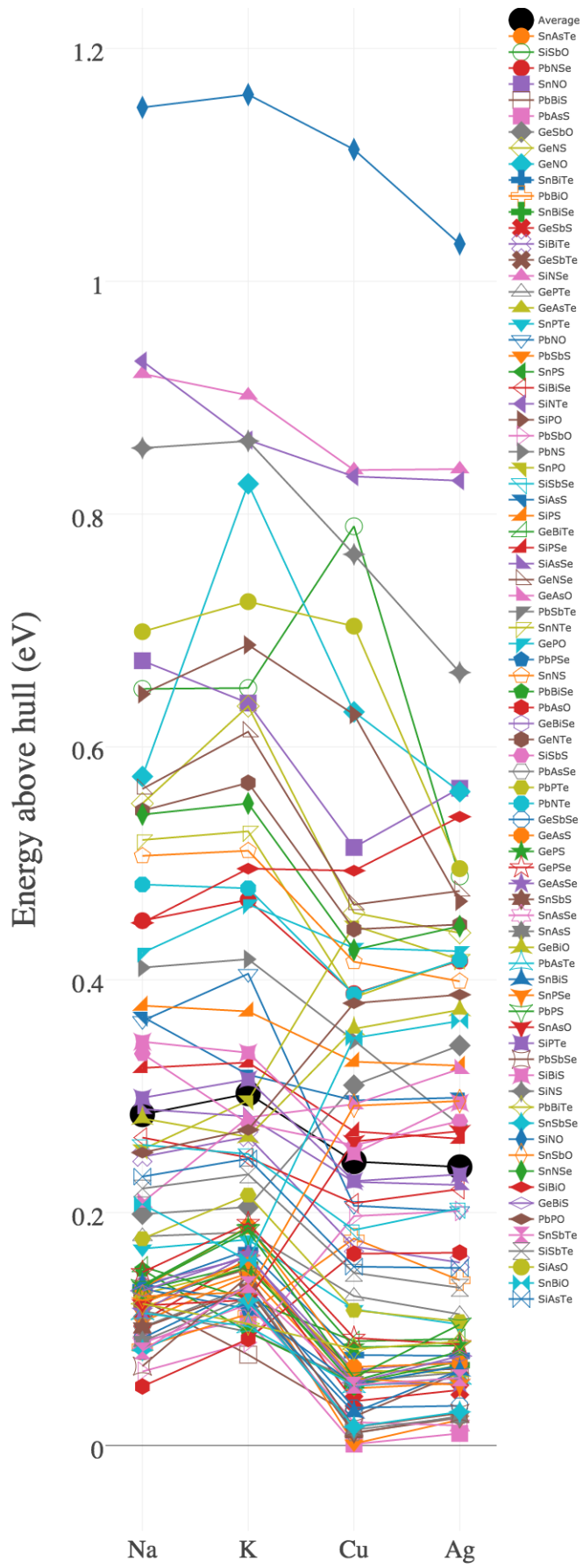
Figure S13. Formation energies of defects in CuPbSbS3 including extrinsic impurities Sn on Sb and Sn on Pb in different regions of phase diagram followed by the chemical potential in eV of each element in this region:

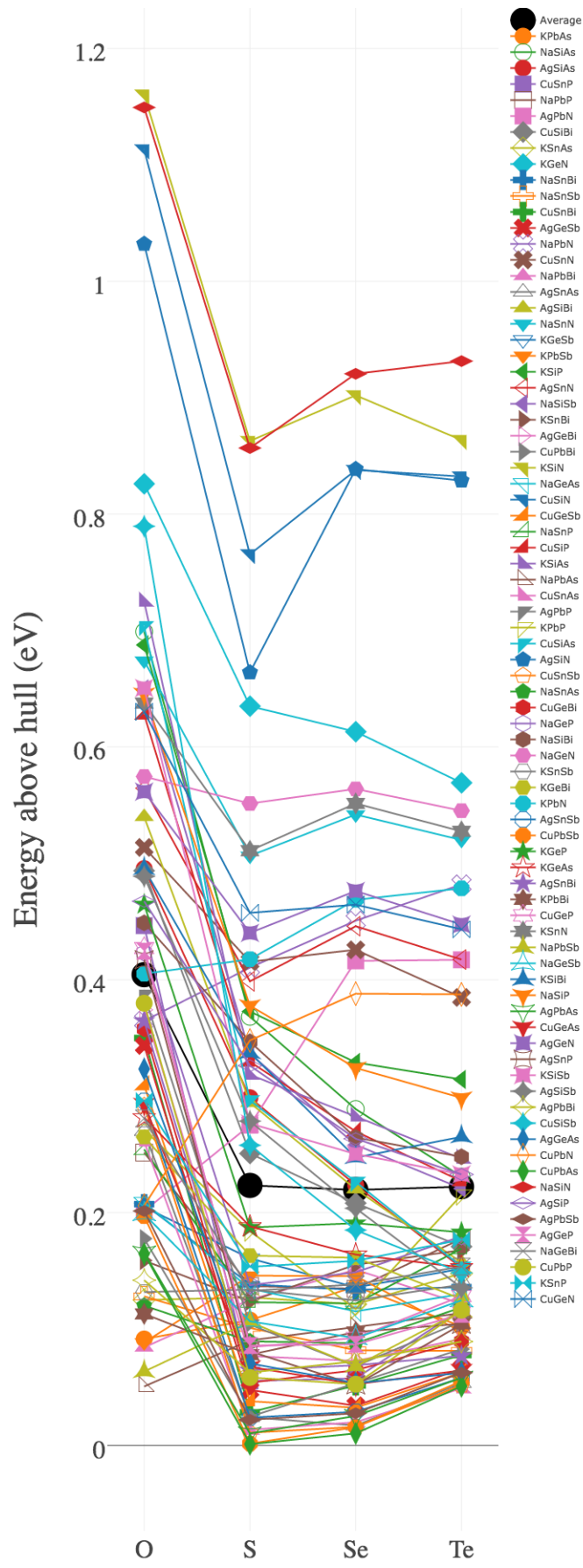
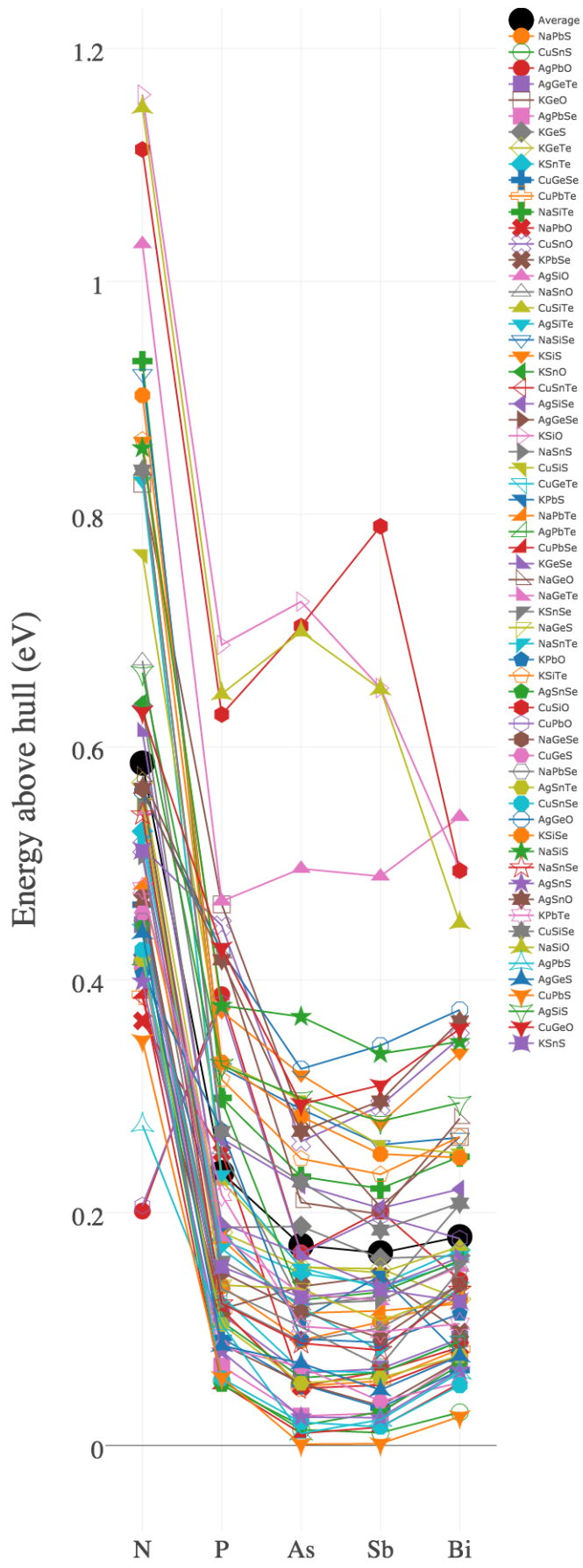
- (a) $\text{Cu}_2\text{SnS}_3\text{-Cu}_{12}\text{Sb}_4\text{S}_{13}\text{-CuSbS}_2\text{-Cu}_3\text{SbS}_4\text{-PbS}$ {Pb: -4.501, Sb: -4.41, S: -4.413, Sn: -4.867, Cu: -4.233}
- (b) $\text{Cu}_2\text{SnS}_3\text{-Cu}_{12}\text{Sb}_4\text{S}_{13}\text{-CuSbS}_2\text{-Sb-PbS}$ {Pb: -4.293, Sb: -4.124, S: -4.621, Sn: -4.503, Cu: -4.103}
- (c) $\text{Cu}_2\text{SnS}_3\text{-Sb}_8(\text{PbS}_5)_3\text{-CuSbS}_2\text{-Cu}_3\text{SbS}_4\text{-PbS}$ {Pb: -4.614, Sb: -4.523, S: -4.3, Sn: -4.98, Cu: -4.346}
- (d) $\text{Cu}_2\text{SnS}_3\text{-Sb}_8(\text{PbS}_5)_3\text{-SnS-CuSbS}_2\text{-PbS}$ {Pb: -4.359, Sb: -4.141, S: -4.555, Sn: -4.47, Cu: -4.218}
- (e) $\text{Cu}_2\text{SnS}_3\text{-SnS-CuSbS}_2\text{-Sb-PbS}$ {Pb: -4.342, Sb: -4.124, S: -4.571, Sn: -4.454, Cu: -4.202}
- (f) $\text{Sb}_8(\text{PbS}_5)_3\text{-SnS-CuSbS}_2\text{-Sb-PbS}$ {Pb: -4.348, Sb: -4.124, S: -4.566, Sn: -4.459, Cu: -4.213}

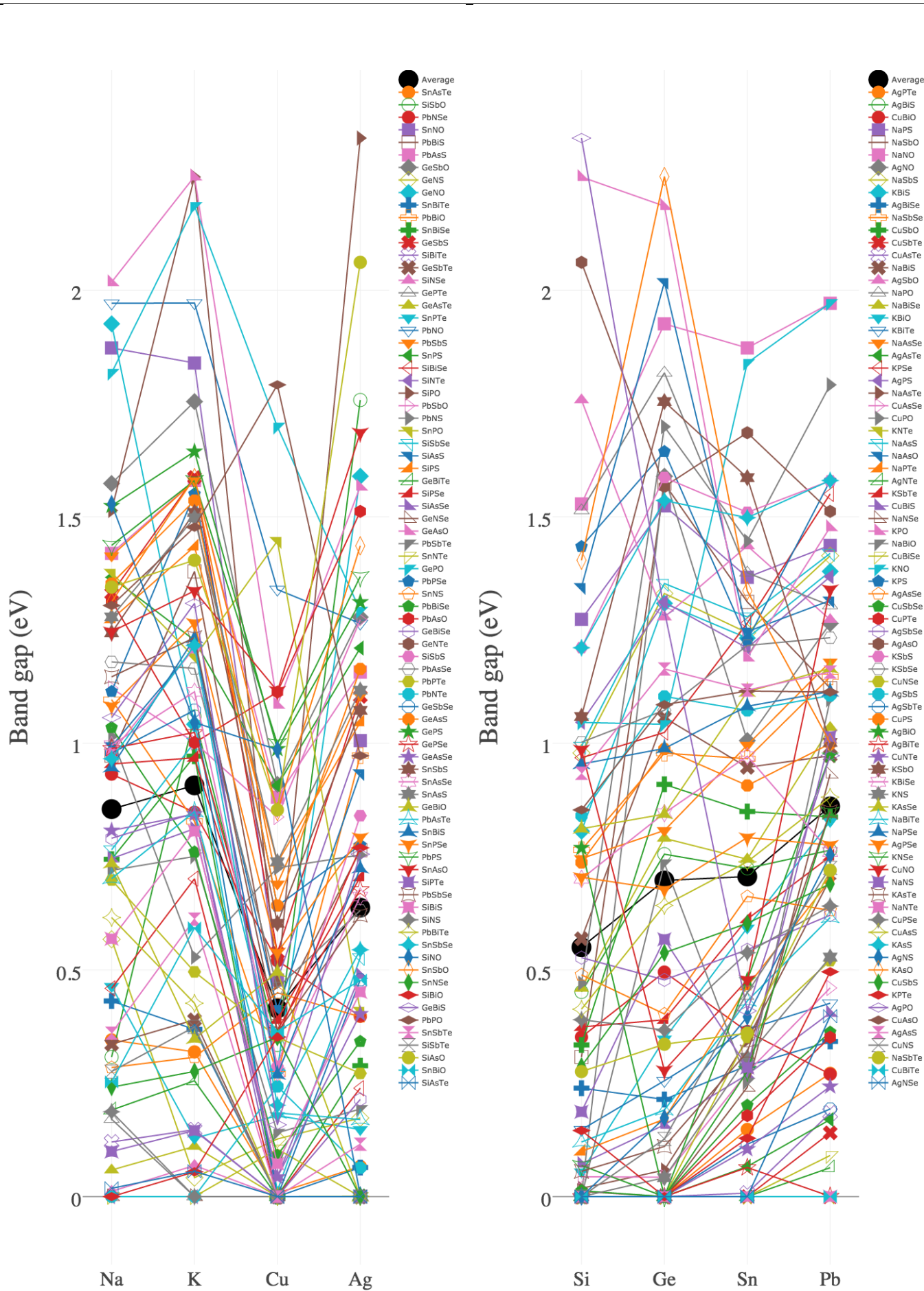
4 Intra-group changes in properties (detailed): E_{form} , E_h , E_g , n -PF, p -PF

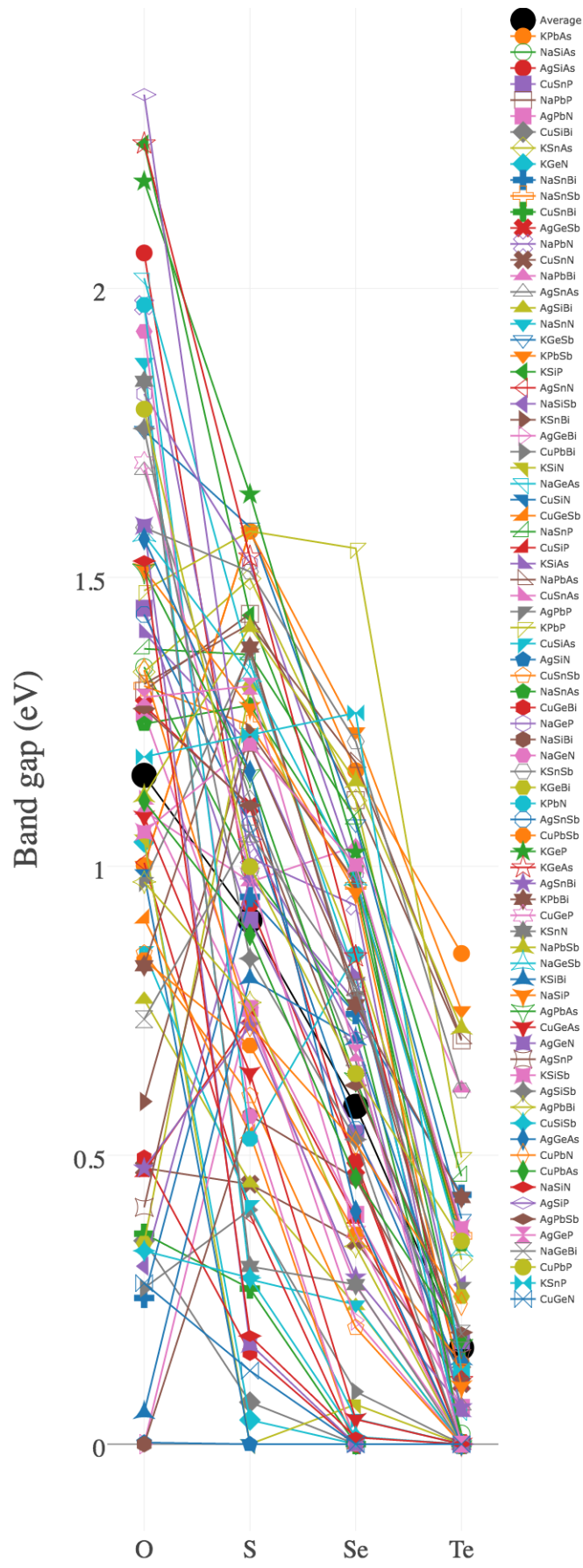
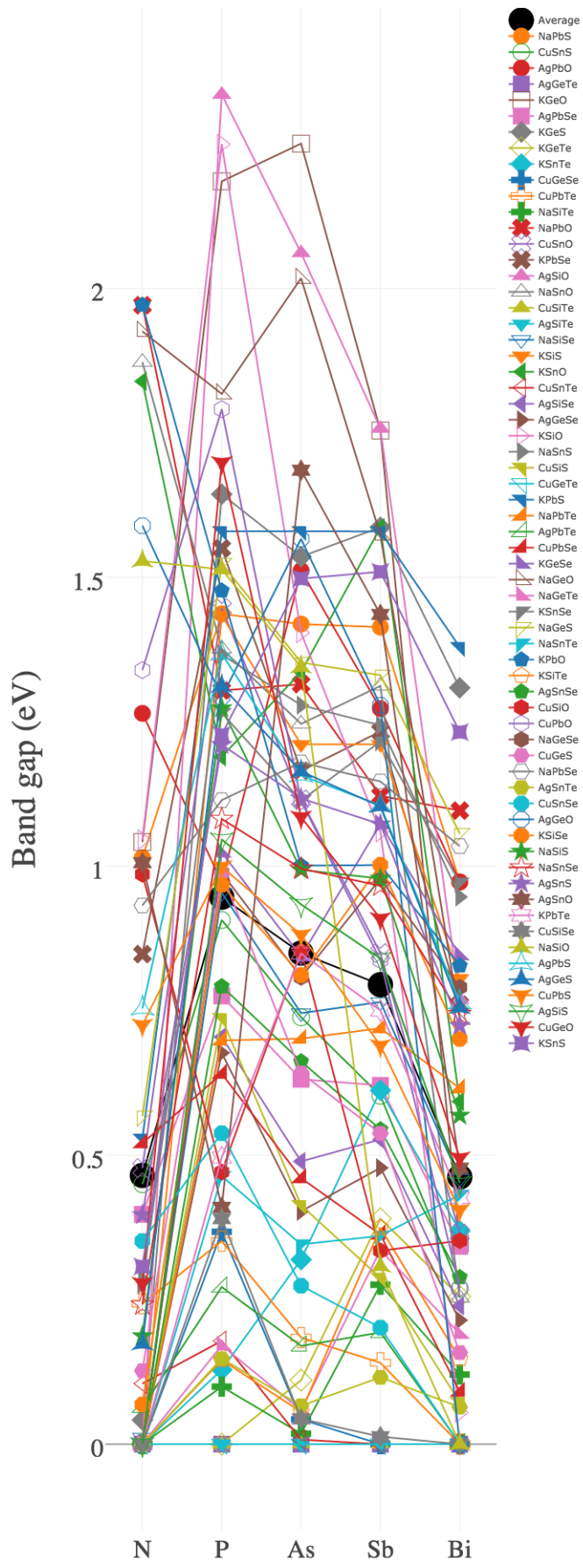


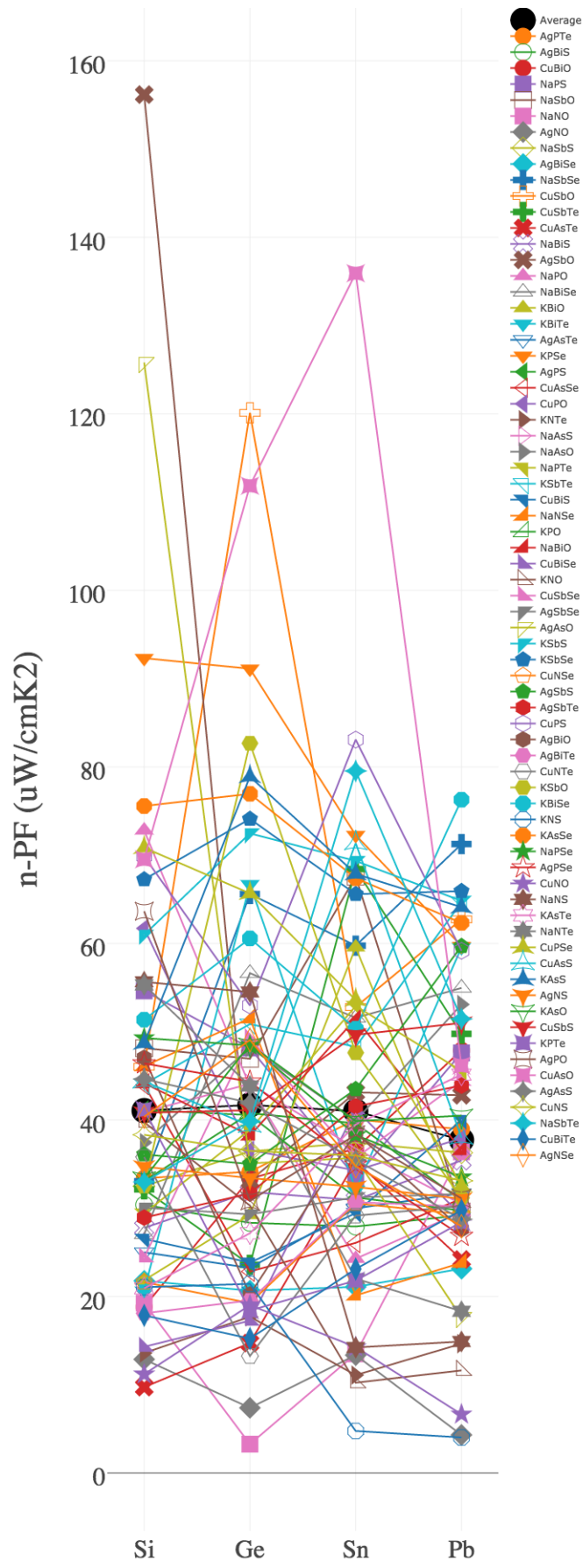
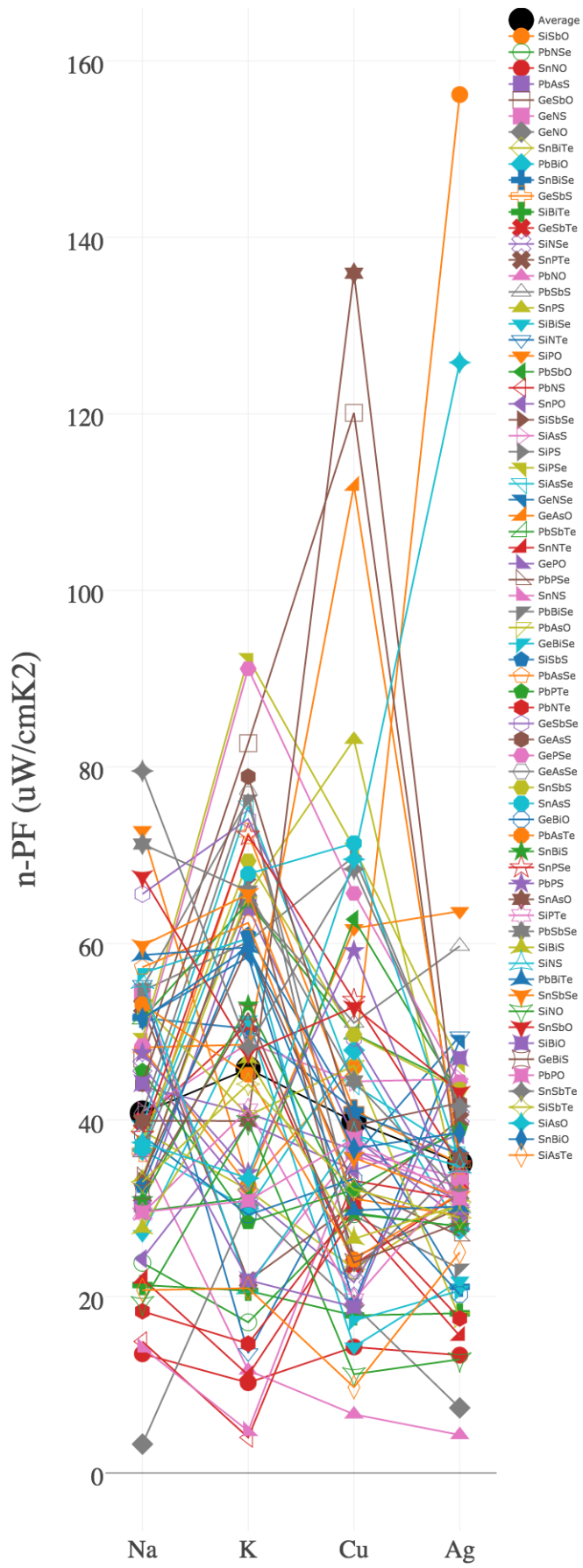


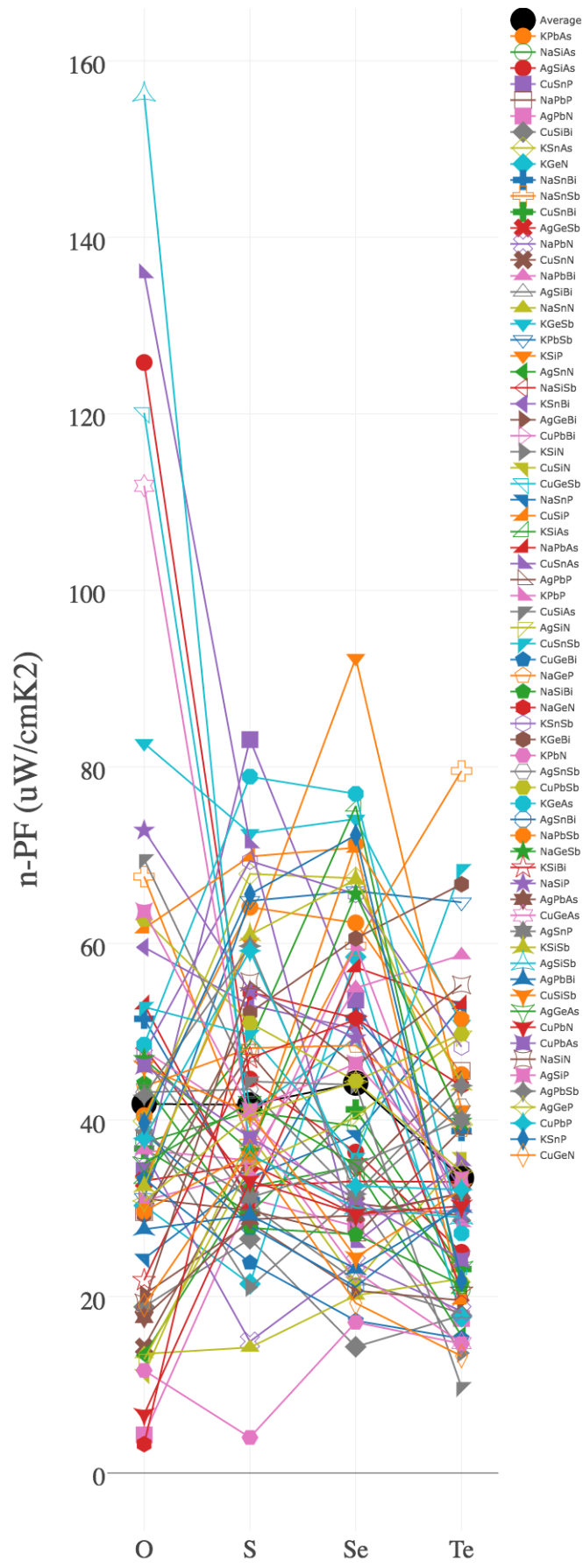
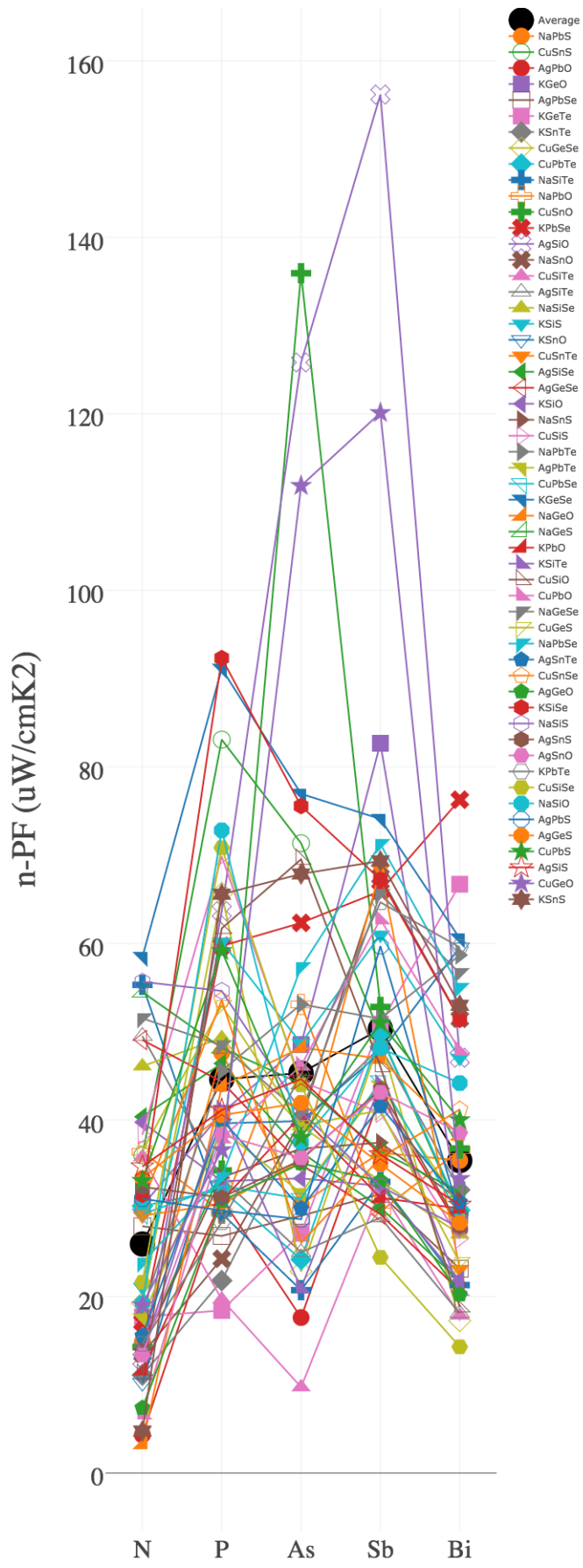


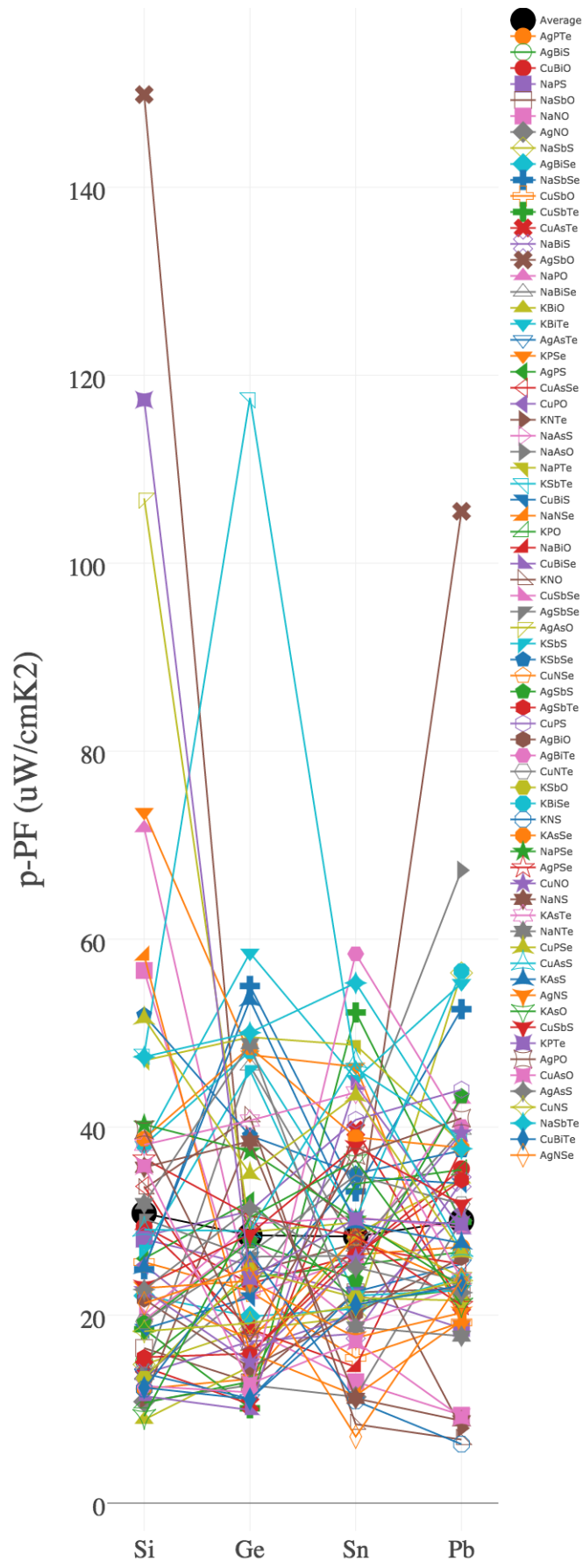
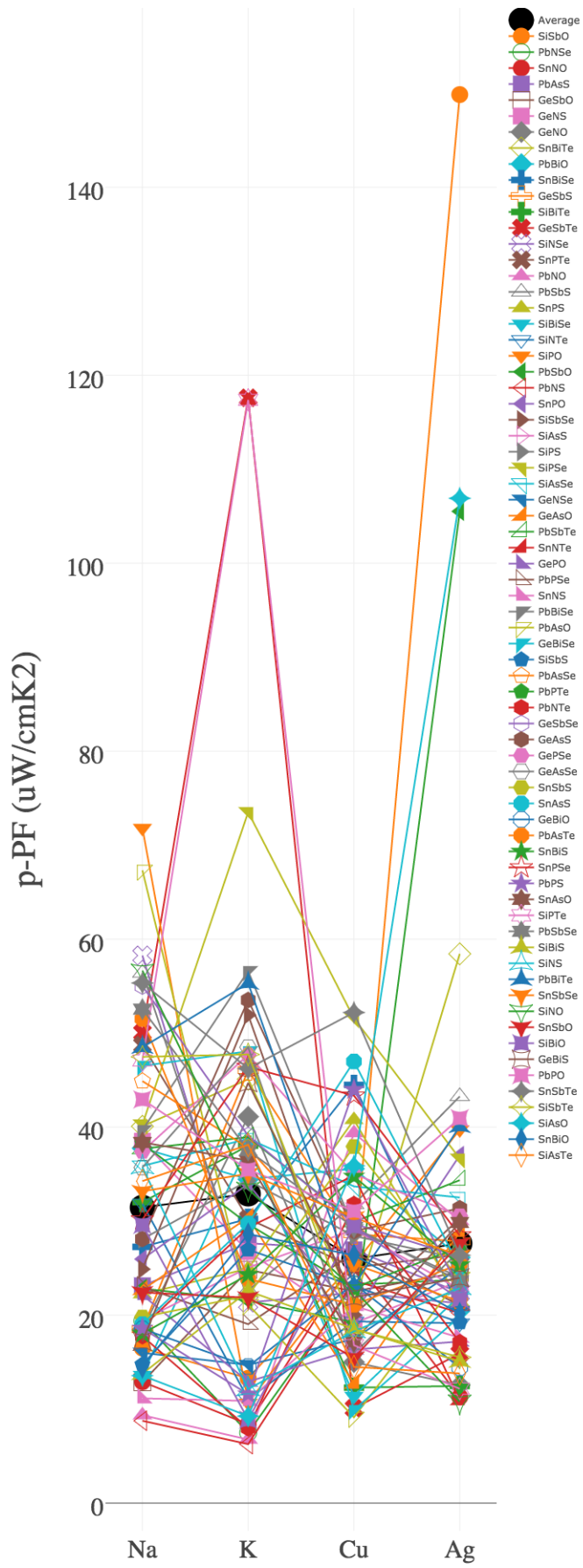












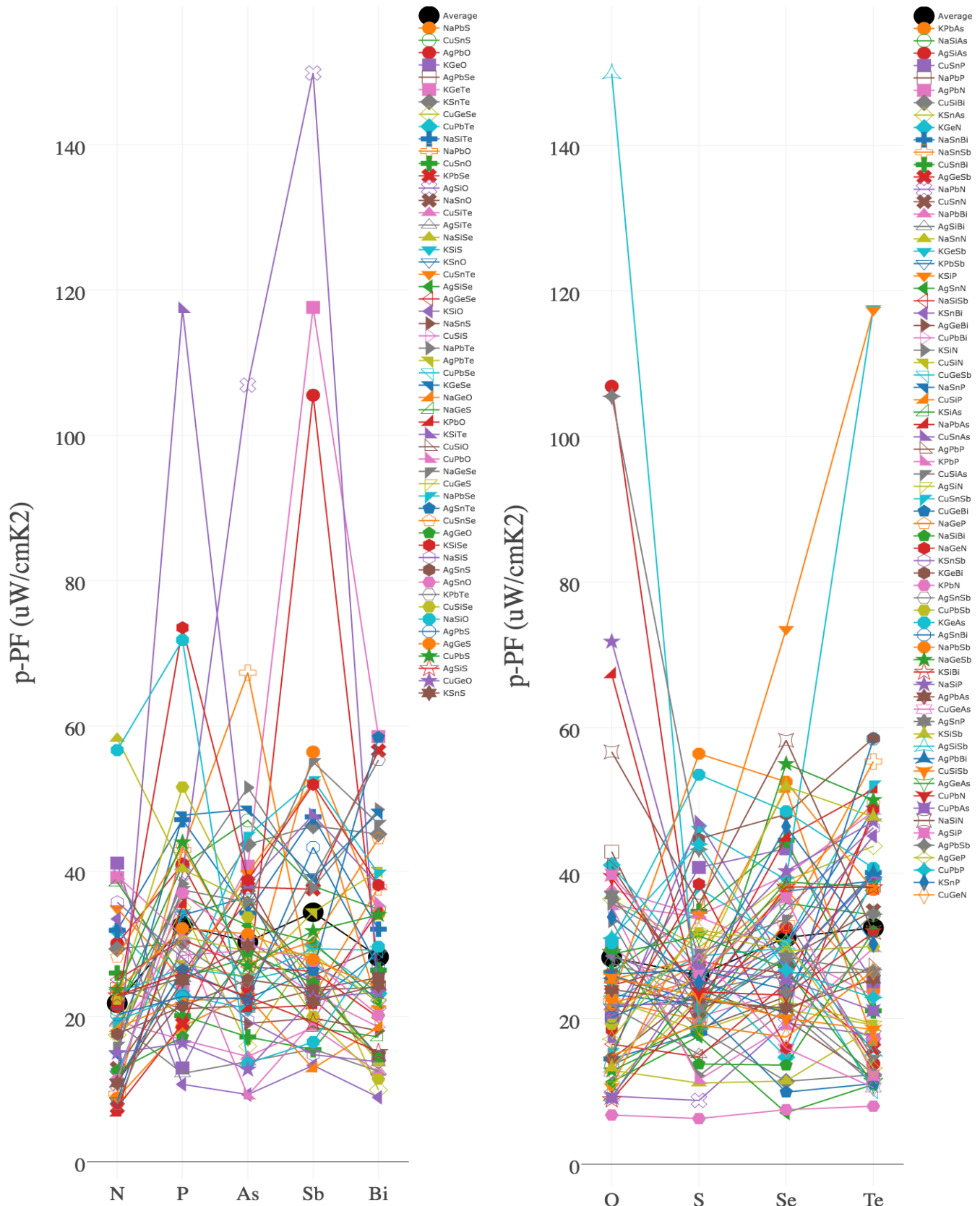


Figure S14. Detail plot of all properties across different groups of elements. Units of formation energy and E above hull are eV/atom

5 Comparison of predicted transport properties via AMSET and BoltzTraP

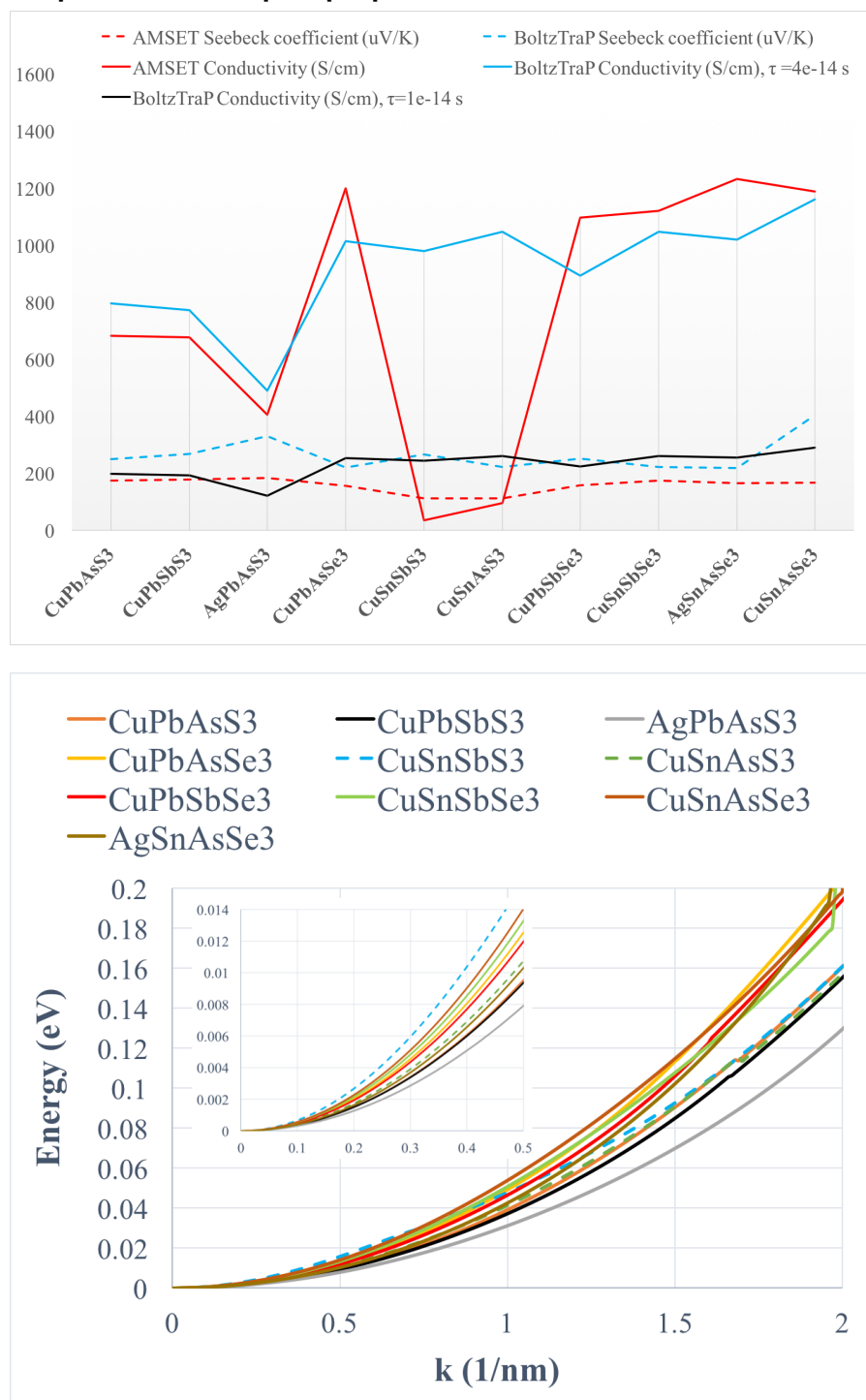
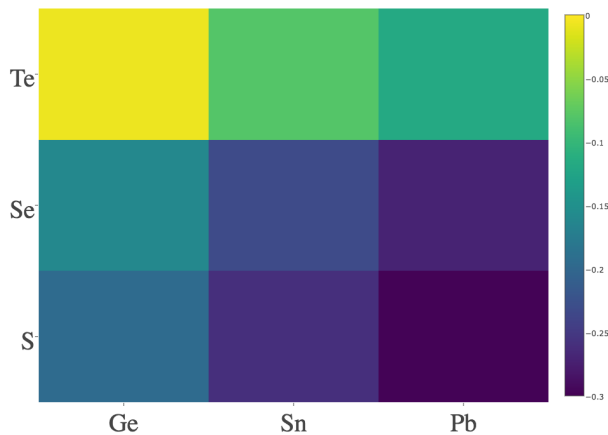


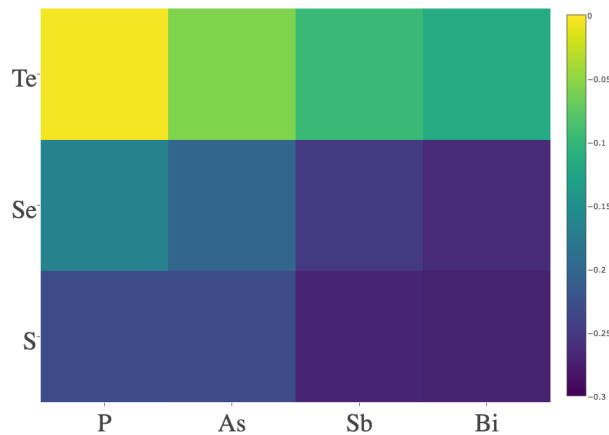
Figure S15. Comparing AMSET and BoltzTraP calculated conductivity and Seebeck coefficient that were used to calculate the power factors reported in Table 1. On top, the original calculated data (from Table 1) is presented plus the BoltzTraP conductivity if $\tau = 4.0 \times 10^{-14}$ s instead of 10^{-14} s which was originally assumed. Bottom plot: the fitted top valence bands in AMSET with R^2 higher than 0.99 in all the cases; the order of the calculated conductivity values have the same order as the slope of the valence bands (proportional to the group velocity) except CuSnSbS₃ and CuSnAsS₃ with very low AMSET conductivities. The reason for that is the inter-band scattering that is present in the two degenerate valence bands in these two compounds as discussed in the manuscript. The inset is a plot of the valence bands zoomed in for better illustration.

6 Heatmaps: how properties change within two groups

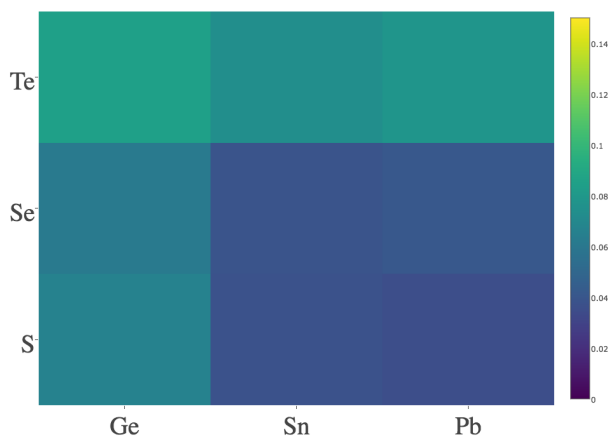
Cu Ag , P As Sb Bi fixed: formation energy



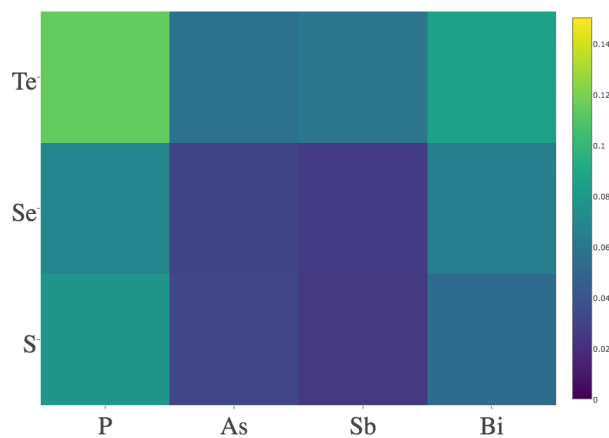
Cu Ag , Ge Sn Pb fixed: formation energy



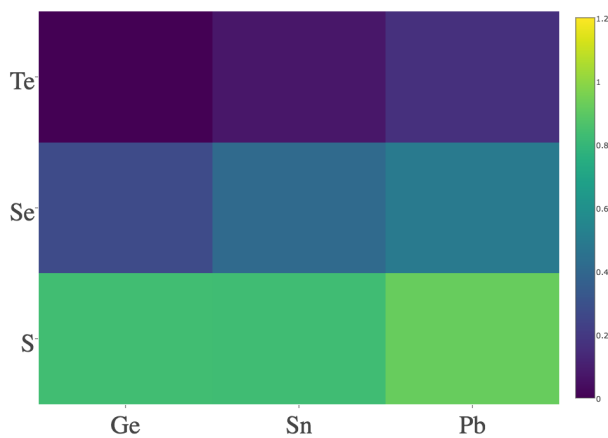
Cu Ag , P As Sb Bi fixed: E above hull



Cu Ag , Ge Sn Pb fixed: E above hull



Cu Ag , P As Sb Bi fixed: band gap



Cu Ag , Ge Sn Pb fixed: band gap

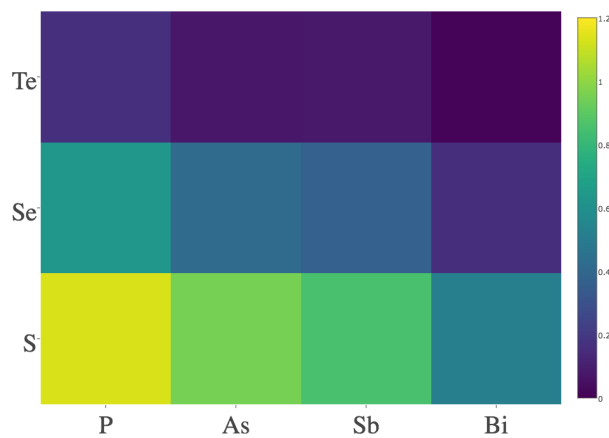


Figure S16. How average properties change with (left) *B* and *D* and (right) *C* and *D* excluding Na, K, Si, N and O.